Palestine Polytechnic University

Deanship of Graduate Studies and Scientific Research

Master of Civil Engineering

Numerical investigation Of Reinforced Concrete Deep Beam With Web Opening Strengthen With Ultra High Performance Concrete

Done By
Rany Imad Mohammad Milhem

Supervisor
Ph.D. Abdulsamea Halahla

Thesis submitted in partial fulfillment of requirements
of the degree Master of Civil Engineering

June, 2023

The undersigned hereby certify that they have read, examined and recommended to the Deanship of Graduate Studies and Scientific Research at Palestine Polytechnic University:

[Numerical investigation Of Reinforced Concrete Deep Beam With Web Opening Strengthen With Ultra High Performance Concrete]

[Rany Imad Mohammad Milhem]

In partial fulfillment of the requirements for the degree of Master in Civil Engineering.

Graduate Advisory Committee:

Graduate Advisory Committee:

Prof./Dr. …… University …,……..

Signature:———————————— Date:————————

Prof./Dr. …… University …,……..

Signature:———————————— Date:————————

Prof./Dr. …… University …,……..

Signature:———————————— Date:————————

Prof./Dr. …… University …,……..

Signature:———————————— Date:————————

Thesis Approved by:

Name:

Dean of Graduate Studies & Scientific Research

Palestine Polytechnic University

Signature:……..……

Date:…..……...……

[Numerical investigation Of Reinforced Concrete Deep Beam With Web Opening Strengthen With Ultra High Performance Concrete]

(Rany Imad Mohammad Milhem)

ABSTRACT

Deep beam is an important structural element that have recently increased in use in concrete buildings, such as tall buildings to offshore gravity structures . We often need to make web opening in Deep beam . These openings reduce the maximum bearing capacity of the deep beam , that why we need to strengthen it , There are several strengthen materials in this research we will use Ultra High Performance Concrete (UHPC) .

In this thesis , I study five reinforcement concrete Deep beam , one is control without web opening and other with web opening , from "Jasim, W. A., et al. (2018)" numerically by ABAQUS , comparing the results Experimental test with ABAQUS result , After approving the results of the program same with Experimental test . I put my parameter " UHPC thickness 30mm & 20 mm and location of the layer at full grove face two side , four layer two for each side , and effect of no shear stirrups " , properties of UHPC from [Bahraq, Ashraf Awadh, et al. 2019}.

The result is , web opening reduce ultimate failure load 27% average . Displacement for deep beam with web opening at edge span is greater than at mid span 15% for the same open size . Used UHPC as strengthen material is good and increase the ultimate failure load 20-37% for deep beam with web opening . Shear bars can replaced by full UHPC layer from two face with 30mm minimum depth and gave more ultimate load and displacement .

التحقيق العددي في السلوك المرن والقص لتقوية الجسور الخرسانية العميقة المسلحة بخرسانة فائقة الأداء

راني عماد محمد ملحم

المستخلص:

الجسر العميق هو عنصر انشائي مهم زاد استخدامه مؤخرا في المباني الخرسانية ، مثل المباني الشاهقة و ابار المياه و الجسور . غالبا ما نحتاج إلى عمل فتحات في الجسور العميقة . هذه الفتحات تقلل من قدرة تحمل الحد الأقصى للجسر العميقق ، وهذا السبب في أننا بحاجة إلى تعزيزه ، وهناك العديد من مواد التعزيز في هذا البحث سوف نستخدم الخرسانة فائقة الاداء .

في هذه الأطروحة ، أدرس خمسة جسور عميقة من الخرسانة المسلحة ، جسر بدون فتحات و البقية بفتحات ، من تجربة " Jasim, W. A., et al. (2018) " عدديا باستخدام برنامج الاباكوس ، تم مقارنة نتائج الاختبار التجريبي مع نتيجة أباكوس ، بعد ان حصلنا على نتائج متقاربة استعملت المتغيرات الخاصة بي . تم استعمال خرسانة فائقة الاداء كتقوية بسمك 30 ملليمتر و 20 ملليمتر , و تم استعمال موقعان للتقوية على طول العينة من جهتين و حول الفتحة من باربع طبقات طبقتين من جل جهة ، وتأثير ازالة حديد القص من الجسر " .

و كانت النتيجة , وجود الفتحات تقلل قدرة تحمل الجسر بمتوسط 27% . يكون إزاحة الجسر العميق مع فتحات عند امتداد الحافة أكبر من المنتصف بنسبة 15٪ لنفس الحجم الفتحة. تستخدم الخرسانة فائقة الاداء لتقوية الجسر العميق و زيادة حمل الفشل النهائي 20–37٪ للجسر العميق مع فتحات. يمكن استبدال قضبان القص بطبقة كاملة من الخرسانة فائقة الاداءعلى الوجهين مع عمق 30 .

DECLARATION

I declare that the Master Thesis entitled" Numerical investigation Of Reinforced Concrete Deep Beam With Web Opening Strengthen With Ultra High Performance Concrete" is my own original work, and herby certify that unless stated, all work contained within this thesis is my own independent research and has not been submitted for the award of any other degree at any institution, except where due acknowledgement is made in the text.

Student Name: Rany Imad Mohammad Milhem

Signature:———————————— Date:————————————

DEDICATION

Thanks be to God Who is always helping us to success

To my wife & sweet daughter

To my parents ,brother and sisters

To all friends and colleagues

To my teachers

To all of them

ACKNOWLEDGEMENT

I would like to thank my supervisor Ph.D. Abdulsamea Halahla for his continuous support and motivation while preparing this work. Ph.D. Belal Almassri the head of the Civil Engineering Department who worked hard to establish the plan for the Master's Degree in Civil Engineering. Ph.D. Haitham Ayyad and Ph.D. Maher Amro who I learned so much from their knowledge.

Contents

Table of figures

Table of tables

Chapter 1: Introduction

1-1 General

Deep beam is an important structural element that have recently increased in use in concrete buildings, such as tall buildings to offshore gravity structures Figure 1 show some deep beam applications. Deep beam is deferent than general beam, and ignoring this difference during design leads to a lack of correct analysis and inaccurate load capacity calculation and the emergence of irregular cracking patterns. It is expected that the problem becomes more complex and the forms of cracks and failures change with openings and their different sizes, locations and numbers, and the bearing capacity of deep beam decreases with the openings.

Reinforced concrete deep beams defined as the main structural component used in buildings and bridges to transfer heavy loads and they are commonly used for transfer girders in tall buildings, foundations (like pile caps and wall footing)

According to ACI 318-19 , a deep beam is a structural component whose clear span is four times the total depth or less or one that has applied point loads that are located within two times the depth or less of the support's face.

According to [Varghese et al., 1966] A "deep beam" is one that has a depth to span ratio (a/d) that is high enough to cause nonlinearity in the elastic flexural stress distribution throughout the depth of the beam and non-parabolic shear stress distribution. [Varghese et al., 1966]. In the shear span, the interaction of bending and shear forces causes inclined fractures that turn the beam into a tied-arch [Yagendra, 1976].

Opening in the deep beam is important in some buildings for air conditioners, electricity pipes, or computer and network cables. that's why a lot of researcher's study opening in the deep beam in the previous year. Sometimes open made with the core is important to determine the properties of the structural element. Researchers found that opening reduces the capacity of the beam and must be studied. [Campione et al.2012]

Structural elements need to be strengthened and rehabilitated for several reasons: the presence of holes in the structural element , the age of the structure , corrosion in the iron or I miscalculate the loads or the element loaded with more than its ultimate load (Altin et al. 2005). . The researchers used different materials to strengthen and rehabilitation such as fiber reinforced polymer (FRP), Ultra-high-performance concrete (UHPC), carbon fiber reinforced polymer (CFRP), shape memory allow Where each material has characteristics and ways to fix it to the element (Chen and Teng 2003). The researchers found many problems and weaknesses in the CFRP and FRP as low fire resistance, fading bonding ... etc.

Ultra-high-performance concrete (UHPC) is characterized by its excellent physical and mechanical properties. Studies have shown that it has various characteristics such as high ductility, flexural strength, toughness, and fracture energy. Compared to conventional concrete, UHPC's ductility is over a hundred times greater.

Ultra-high-performance concrete (UHPC) is considered a modern material and is distinguished from other reinforcing materials by a high ability to resist fire and easier bonding with the element (Li 2004). Ultra-High-Performance concrete, is a new material that used to strengthening R.C. element that consist of cementitious materials, high tensile fiber, and little amount of water (Al-osta 2018). Ultra-high-performance concrete (UHPC) defines it as a cement-concrete material mixed with fiber, which has the characteristics of durability, tensile strength and a compression strength at least 120 MPa (B.A. Graybeal 2009).

In this research we will use Ultra-high-performance concrete (UHPC) as a layer around the opening in deep beam to strength it and study that effect , this study will be the first one use UHPC to strength open , other researcher use CFRP , FRP , and other strengthen material or use Ultra-high-performance concrete deep beam alternative to ordinary concrete deep.

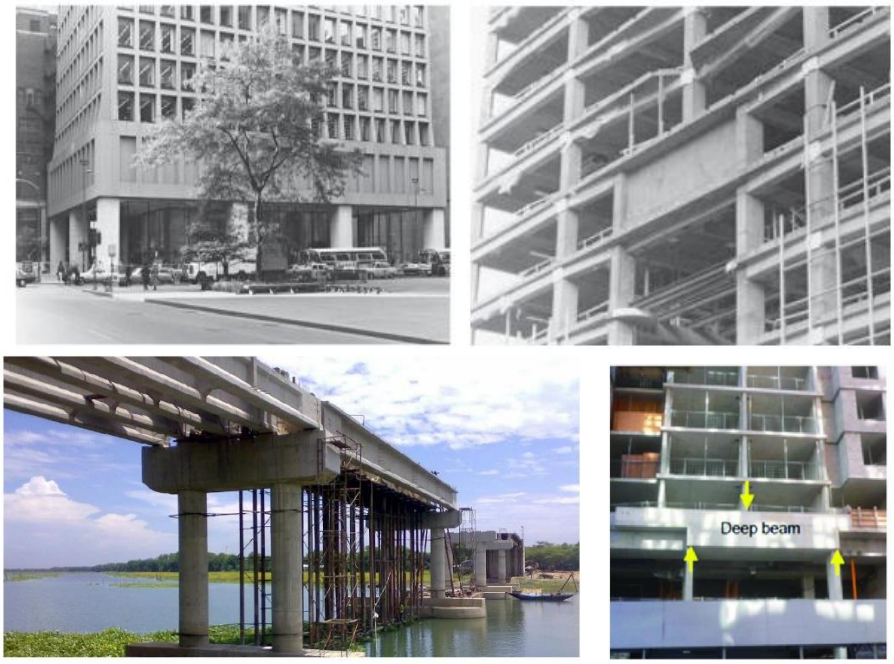

Figure 1 :deep beam applications

1-2 BEHAVIOR OF DEEP BEAMS

In order to resist flexural and shear stresses, RC components are built using the premise that strains change linearly in section. For the general beam in elastic zone, the mechanical behavior depends on Bernoulli's hypothesis " planar sections remain plane after the load has applied " Yagendra, 1976.

Any structural member can be split into two regions:

* B-regions shown in Fig(2) in section A-A at the member parts where beam theory can be applied (Bernoulli theory), the sectional method can be used to find stress value .
* D-regions showed in Fig(2) in section B-B at that region Bernoulli theory invalid and known as (Discontinuity region or Deep beam region), the behavior is controlled by shear strains. Frequently, sudden changes in loading or changes in geometry result in nonlinear strain distributions. If shear-span-to-depth ratio is less than 2-2.5 (where 2 for simply supported beam and 2.5 for continuous beam) the behavior of the beam is a deep beam, if a/d is greater than 2.5 the behavior of the member according to sectional principle. D-regions occur at concentrated loads, corners, bends, openings, and other discontinuities.

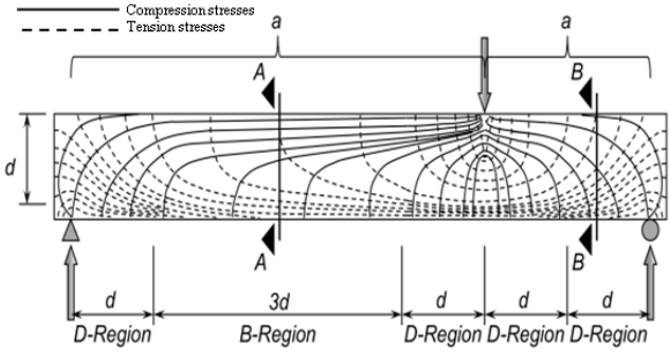

Figure 2: Stress path in B and D region [tuchscerer et al.2011]

1-3 MODES OF FAILURE OF REINFORCED CONCRETE DEEP BEAMS

1-3-1 Modes of Failure of Deep Beams without Web Openings

The web splitting force and the strength capability of the primary reinforcement determines the deep beam's mode of failure. Three modes of failure can occur:

Mode 1: Flexure: this type of failure is rare to happened. Low bottom steel content causes the mid-span tension failure of the beam. As shown in Figure (3).

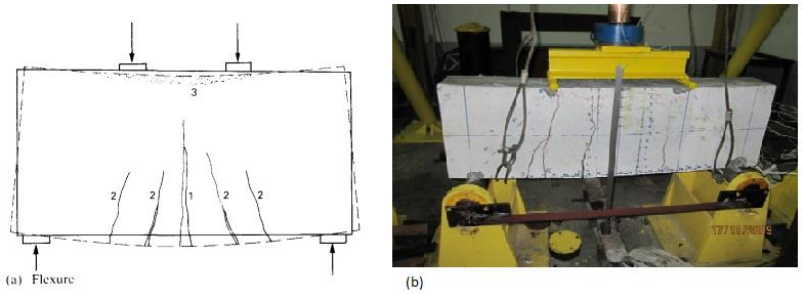

Figure 3:Flexure failure, (a) failure of deep beams [Subedi et al 1986] , (b) [Mohammadhassani 2012]

Mode 2: Flexural shear: In this type there is a good amount of bottom steel, main failure in shear and occurs at the support upwards towards the load, Flexural cracks often appear at mid-span before the shear cracks develop. As shown in Figure (4).

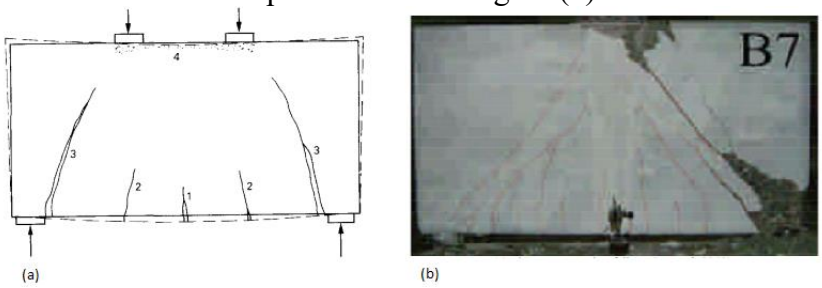

Figure 4:Flexure shear failure, (a) failure of deep beams [Subedi et al 1986] , (b) [lu et al. 2013]

Mode 3: Diagonal splitting failure: Is consider the most frequent mode of failure. Similar to the first two failure types, the third shear fracture also spans between a load and a support, but this time it begins more brittle and spreads outward from midspan. As shown in Figure (5)

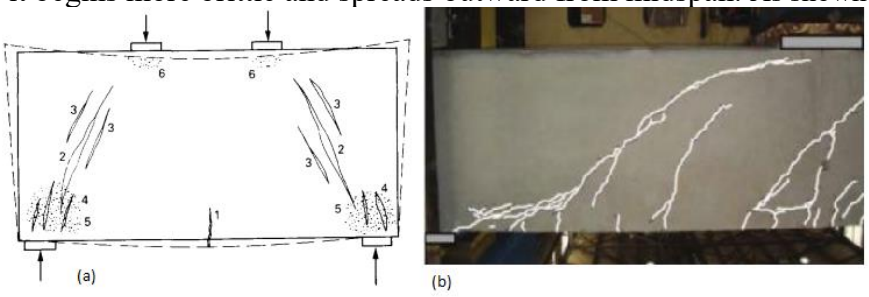

.

Figure 5: Diagonal splitting, (a) failure of deep beams [Subedi et al 1986] , (b) [Diagonal tension failure (Birrcher et al. 2013)]

1-3-2 Modes of Failure of Deep Beams with web Openings

The ACI Code and other current standards of practice don't provide specifications for web openings in deep beams. There are three modes of failure in deep beam, [Mansur and Alwis, 1984] are classified these modes depending on the failure shape.

Mode A: in this type of failure the crack goes diagonally from the reaction point to support. Shown in Figure (6).

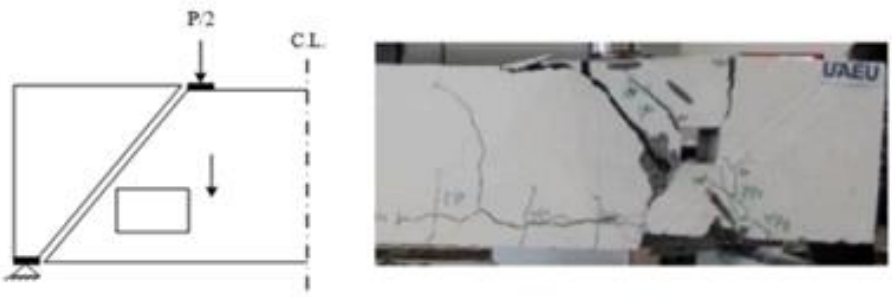

Figure 6: mode A failure, failure of deep beams left [Mansur and Alwis, 1984], right [Mansour, M., & El-Maaddawy, T. (2021)]

Mode B: This type occurs as a result of a sudden fracture. It consists of the edge of the opening to the loading point and to the support. Shown in Figure (7).

Figure 7: mode B failure, failure of deep beams left [Mansur and Alwis, 1984], right [jasim et al 2020]

Mode C: It comes from deformation mostly in the shear span with relative rotation of three separate beam segments. Normally occurs gradually. Shown in Figure (8).

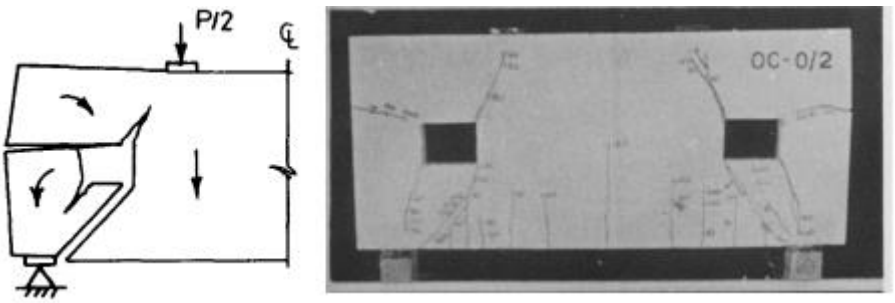

Figure 8: mode C failure, failure of deep beams left [Mansur and Alwis, 1984][18], right [Mansur and Alwis, 1984][18]

1-4 Research Significance and objectives

- Increase ultimate failure load for deep beam with large web open
- Exploring the best location, dimension and thickness of the ultra high performance concrete .

1-5 Methodology

Numerical Analysis will be used for this study. “ ABAQUS ” software will be hired to model the deep beam subjected to loads cause some deformation, this deformation will be treated and analyzed by Finite Element Method (FEM).

Chapter 2: LITERATURE REVIEW

2-1 General

This chapter reviews the properties of deep beams with and without openings, and methods of strengthening them. With the development in the engineering field, the use of deep beam has increased, especially those with openings (whether used as ventilation holes or doors ... etc.), there is a lack of explanation and solution of deep beam containing opening in the ACI American code, specially beam strengthen with different strengthen materials like Ultra-High-Performance Concrete UHPC.

We will review a set of previous experimental and theoretical studies that tested a group of deep-beam with opening under the influence of various variables. The most important variables are:

* Effect of the dimension of the opening.
* Effect of strengthening and location of Ultra High-Performance Concrete on Deep Beam (grooved).
* Effect of depth of Ultra High-Performance Concrete layer on Deep Beam (grooved).
* Effect of shear on Deep Beam .

2-2 Strut and Tie Model (STM) for deep beam

2-2-1 General

Strut-and-tie modeling is a tool for reinforced concrete components analysis and design that allows for the assumption that internal stresses are transmitted through a truss mechanism. Or known as a flexible, lower-bound design approach for structural elements made of reinforced concrete. STM used to design D-region (Discontinuity region or Deep beam region), in this region Bernoulli's hypothesis can no longer be use. regional method must use to design D-region, instead of a sectional.

(Wilhelm Ritter et al, 1899) proposed the truss mechanism to describe how transverse reinforcement helps a beam withstand shearing. (Lampert and Thürlimann 1971) created a three dimensional space truss to describe the combined effects of shear and torsion.

(Schlaich et al, 1987) presented the strut-and-tie modeling technique. extended the truss modeling approach for regions with overall discontinuity. The discontinuous D-region is idealized by the strut-and-tie model (STM) as a diagonal compression strut running from the load point to the support point. It is an improved shear design model that makes designing and analyzing concrete buildings simpler (Park, J.W et al.2007).

2-2-2 For deep beam

The Strut and Tie method is the simplest and easiest way to design deep beam. The Strut and Tie method also used to calculate the bearing capacity of other elements such as corbel, deep beam and other discontinuity region member (Lin, I. J. et al. 2003)(Lu, W. Y. et al. 2009).

The Strut and Tie method deal with stress on the member as a flow stress in truss member. Diagonal struts may depict the concrete's flow of concentrated compressive stresses, while tension ties can represent the generated concentrated tensile stresses. Both types of stresses are resisted by steel reinforcement. Where nodal zoon can defend as areas where struts and ties cross each other.

Pre-stressing tendons and steel reinforcing bar can be used for tensile ties. A tensile tie can also be used to describe a concrete tensile stress field. Although axial steel can be used to strengthen the compressive strength of the strut, concrete sections are commonly compressive struts. The equilibrium of the system regulates the amount of forces passing through the compressive struts and tensile ties. Since there are several strut and tie alignments that may be used to represent the load resistance of a structure, the strut and tie approach is not a direct way of design. The least amount of strain on the strut and tie parts will result from the optimal alignment of the struts and ties. The concrete structure is split into two regions: B-regions; Bernoulli hypothesis of plane section, and D-regions where strain distribution is considerably nonlinear. Deep beams are typically thought of as one D-region in their entirety.

2-3 Literature review STM

(Hamid Karimizadeh and Abolfazl Arabzadeh 2021) study deep beam with circular and rectangular web opening analytically using strut and tie model, the practical results of a group of researchers with a total of 121 samples and compare between ultimate load experimentally and ultimate load analytically using flowchart calculation and type of failure. The result was that the suggested model was conservative due to the relatively low load capacity values produced from the analytical model compared to the observed values, which is seen to be advantageous for structural design reasons. The model was shown to be less accurate the greater the load capacity of the specimens. This was explained by referring to the significant number of fractures that make it more challenging to identify the proper truss model that corresponds to the failure mechanism of the beam. The same was shown more clearly in the case of beams without apertures, where the model would lose accuracy since higher resistance levels made the standard truss.

[Tseng et al., 2017] Develop an analytical method to calculate the shear capacity in deep beams containing web openings in order to determine the paths of transmission of shear forces depending on the strut and tie method. The proposed technique has the capacity to forecast several forms of failure, such as splitting, yielding, and crushing of concrete. The compressive strength of the concrete, the reinforcement ratio, the span-depth ratio, and the sizes and placements of the web apertures were all factors taken into consideration in this study. Results from the comparison showed that the suggested approach can measure the shear strength of reinforced concrete deep beams with web opening logically.

[Tan, K. H. et al. 2004] As the derivations differ from the other examples, only the formulations of inclined web reinforcement are offered in this study. This research examines STM for deep beams with web opening analytically and compares the results with previous practical experiments. Eight Samples from (Kong F. K., et al. 1977) had inclined web reinforcement above the web openings. He found that it is more effective to place reinforcement above the opening (Awa) than to place reinforcement in the web below the opening (Awb). According to experimental findings, strengthening above the opening (Awa)

can double the final strength of an opening deep beam, strengthening below the opening (Awb) might add 10% to its strength only.

Park and Kuchma (2007) provided a method based on struts and ties to determine the strength of deep reinforced concrete beams. The suggested approach utilizes secant stiffness formulation, strain compatibility, and constitutive principles for cracked reinforced concrete. The technique took into consideration failure modes caused by strut crushing or splitting as well as those caused by yielding of the longitudinal reinforcement and crushing of the nodal compression zone at the top of the diagonal strut. This approach was used to determine the capacity of 214 deep concrete beams that had undergone laboratory testing for both normal and high strength. The comparison revealed that the suggested technique regularly makes accurate predictions of the shear span to depth (a/d), concrete strengths, and strengths of deep beams with a wide range of horizontal and vertical web reinforcement ratios. The suggested method sheds important light on the construction and operation of deep beams.

2-4 Literature review deep beam

Campione, G., & Minafò, G. (2012) study 20 small scale concrete deep beam experimentally and analytically with circular web opening and low shear span to depth ratio. the variable is opening location and reinforcement arrangement. the result is the opening location The existence and location of the hole largely determine the failure mode and the first cracking stress , the ultimate load is increased by 15% if vertical stirrups is used in solid or mid span open deep beam , horizontal stirrups increase ultimate load 10% if opening within shear span .

[Al-Ahmed and Khalaf, 2017] In this study, nine external post-tensioning strand-strengthened reinforced concrete deep beams with wide web holes have been cast and tested till failure. The findings shown that raising the openings ratio decreased ultimate and first cracking loads while raising mid span deflection for all beams. While adopting the horizontal strengthening method, there is a noticeable reduction in bottom (tension) reinforcement stresses as compared to beams without strengthening at the same load level and at the same openings ratio. The horizontal strengthening plan resulted in an overall strength increase between 32% - 53%. In order to improve the shear strength of RC deep beams, a strategy using externally horizontal prestressed strands was shown to be particularly successful.

(Abuzar Hamzenezhadi et al 2021) study experimentally eight deep reinforced concrete beams that had been cast and replaced with high performance cementitious composites underwent. The test findings showed that changing traditional concrete with cementitious composites containing 2% of steel fiber improved the deep-beam specimens load-bearing capability up to 84.8% with the same diameter.

(Hu et al. 2017) Six deep beams with a trapezoidal aperture in the middle or extending from the middle to the shear span were tested, depending on the size of the aperture, multiple types of failure were discovered, and because of the trapezoidal form, concrete in the corners of specimens with bigger openings showed localized failure, The value of the initial flexural cracking load was altered by the existence of an aperture in the midspan, and its size also had an impact on the diagonal crack width.

(Yang et al. 2006) 32 specimen deep beams with rectangular openings were test concrete strengths, and the shear span-to-depth ratio and opening size varied from 0.5 to 1. Researchers discovered that deep beams with apertures greatly reduced the impact of concrete compressive strength on the load-carrying capacity.

(Yousef et al.2018) verified five UHPC deep beams with changing horizontal and vertical reinforcement ratios (ρsh and ρsv) to discover the minimum requirements of shear

reinforcement. They found that increasing ρsv had a slight effect on the diagonal cracking and the shear strength.

(Rahim, N. I. et al.2020) and (Abdullah Anwar et al. 2020) carried out a total of nine reinforced concrete deep beams with openings strengthened with carbon fiber reinforced polymer (CFRP) and one control beam without an opening have been cast and tested under static four-point bending load till failure. They found that the increase the size of the opening causes an increase in the shear strength reduction by up to 30%. Therefore, the larger the openings, the lower the capability of load carriage.

(Abadel, Aref, et al.2022) carried out an experimental study of shear behavior of UHPC deep beams strengthened with CFRP. All deep beams were tested under four-point loading until failure. The experimental results showed that the shear stirrups effectively contributed to enhancing shear strength, ultimate load, and deformation capacity for NC deep beam. By utilizing the UHPFRC mix, the shear strength of deep beams was upgraded significantly compared with the NC deep beams, but the deformation capacity was reduced.

(Ahmed Ismail el-kassas et al. 2020) The behavior of nine longitudinally-opening reinforced high-strength self-compacted concrete (RHSSCC) deep beams with varying openings in terms of shape, size, and placement was studied. One-sixth of depth and one-quarter of depth side length or circular diameter dimension are employed, along with two forms (square and circular), two opening locations (compression and tension zone), and two shapes. The findings indicate that longitudinal openings reduce the loading capacity of RHSSCC deep beams, that increasing opening size reduces deep beam capacity load, that changing longitudinal opening shape has a minor impact, and that longitudinal openings located in the compression zone caused a greater reduction than openings located in the tension zone.

[Kumar, 2012] Five RC deep beam specimens with a circular web aperture and no shear reinforcement were evaluated under a two-point load. Around two circular holes, shear strengthening using externally bonded fiber reinforced polymer (FRP) was applied. They found that the increasing in strength by using this method of strengthening was ranged between (68 to 125) % compared with beams without strengthening.

[Jasim. et al.2018] study 10 deep beam experimentally with deferent parameter opening location and size and deferent shear span to depth ratio (a/h) (1.1 and 0.9) . the mail object of this experiment to show the effect of large square opening in deep beam . two specimens are control beam without opening , opening have two dimension 200*200 mm and 230*230mm , with 40% and 46% ratio of square opining side to web depth . stiffer behavior increase when opening with small dimension location in shear span. The ultimate load capacity decrease to 66% for deep beam with opening .

Chapter 3: Finite element modeling

3-1 General

It is a set of calculation and modeling operations to simulate and predict the behavior of an element in different conditions by dividing the element into small parts on the basis of balance, compatibility, and stress-strain relationships. And it can be known as a laboratory experiment by computer. This method is used in the absence of laboratories or for the sake of speedy work in the production of samples and studies of the effects on them or the formation of new materials. The accuracy of the results in the program depends on the accuracy of the inputs, the properties of the materials and the correct modeling of the element.

In this chapter, I will rely on two phases: first step, remodeling the laboratory experiment and ensuring the accuracy of the results and inputs of concrete, iron, etc., by comparing them with the results from the practical experiment. Second step , add Ultra High Performance Concrete (UHPC) layer and study the new properties and compare them with the results from the first step.

3-2 From Experimental test

Experimental work take from : Jasim, W. A., Allawi, A. A., & Oukaili, N. K. (2018). Strength and serviceability of reinforced concrete deep beams with large web openings created in shear spans. *Civil Engineering Journal*, *4*(11), 2560-2574.

They study 10 deep beam experimentally , all deep beam have the same dimension 1500*500*150 mm , with two support roller at right and pin at left , and two point applied load . Two deep beam are control specimen and eight other are with opening with deferent size . Opening have two dimension 200*200 mm and 230*230mm , with 40% and 46% ratio of square opining side to web depth respectively . they study deep beam with deferent shear span to depth ratio of 0.9 and 1.1 .

The following is an explanation of specimen descriptor:

* DP : deep beam specimen . *S1 : shear span to depth ratio equal to 1.1 . *S2 : shear span to depth ratio equal to 0.9 . *C : opening location to the shear span at the center . * E : opening location to the shear span at the interior edge . *O1 : opening size 200*200 mm. *O2 : opening size 230*230 mm. *F : Full face grove Strengthen by UHPC layers (ABAQUS). *G : grove layer around opening from two face with dimension 370*500 mm . *SH : no shear in the supported area . *20 : thickness of UHPC layer is 20 mm . *30 : thickness of UHPC layer is 30 mm .

Table 1 : Material properties

Material

Concrete (Average)	Fc’	27	MPa
Steel Ø 16 mm	Fy	569.67	MPa
Steel Ø 6 mm	Fy	623.96	MPa

The reinforced steel bar used 3Ø16 mm longitudinal bars , Ø6 mm@ 86 mm horizontal bar , Ø6 mm@ 86 mm vertical stirrups .

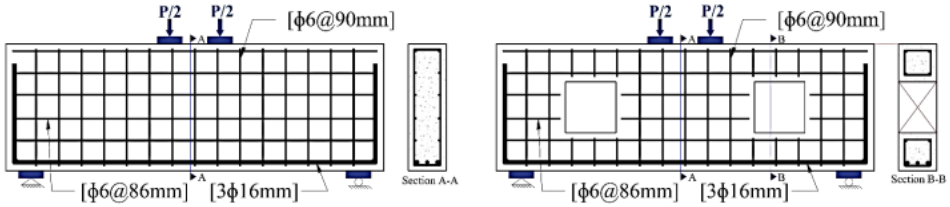

Figure 9 : Experiment specimen reinforcement details

3-2-1 Modeling reinforced concrete deep beam

*Creating parts

This part includes defining the deep beam components separately. All part defined as 3D model space and deformable type . The concrete deep beam , UHPC, supports , and load plate defined as solid – type extrusion . longitudinal and stirrups reinforcement are defined as wire .

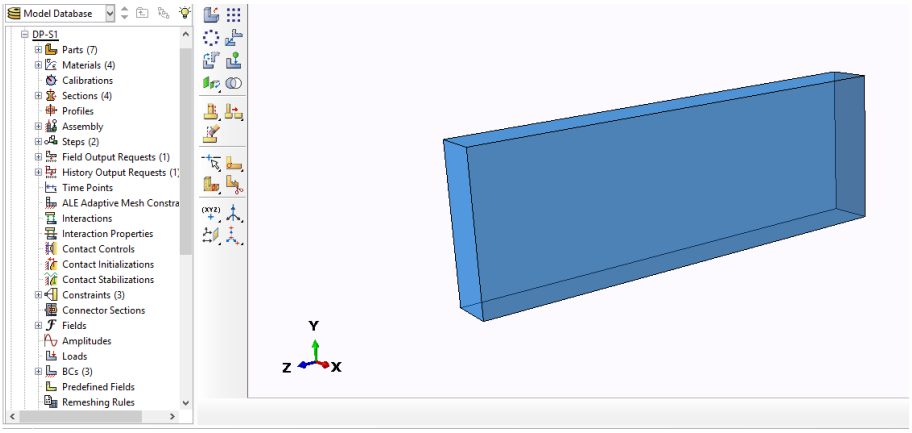

Figure 10:concrete deep beam solid part created (with 1500mm length*500mm depth*150mm width)

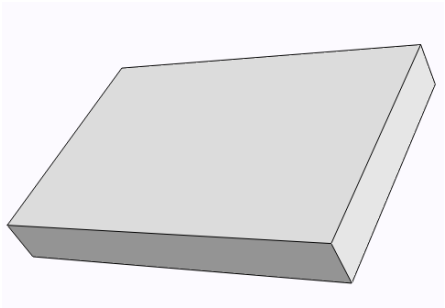

Figure 11: load and support plate are defend as steel solid plate(with dimension 150mm*100mm*20mm)

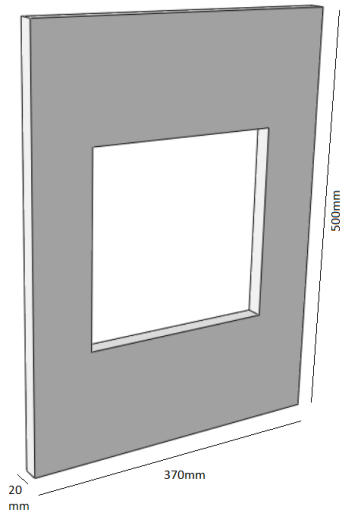

Figure 12 : UHPC layer around the opening dimension (370*500*20&30mm)

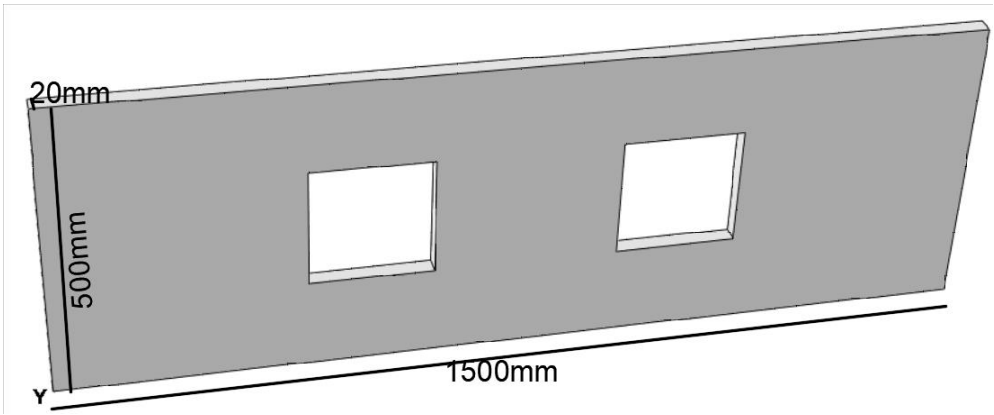

Figure 13:Full UHPC layer with dimension (1500*500*20mm) with opening

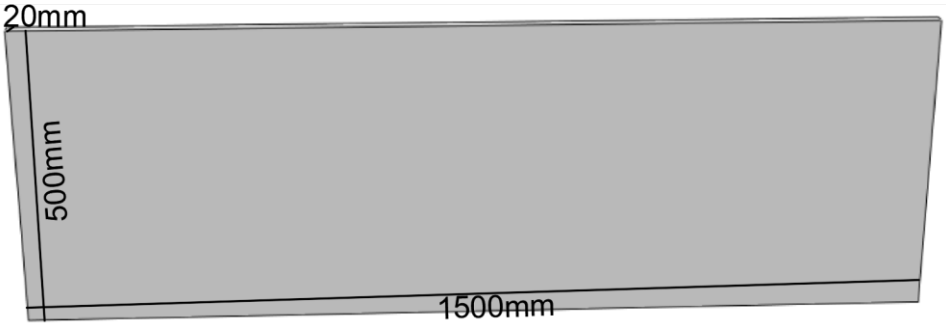

Figure 14 : Full UHPC layer dimension (1500*500*20)without opening

3-2-2 Materials Properties

* The reinforced steel are defined as an elastic completely plastic material isotropic type . The elastic property for young modulus =200*10^5 MPa and poisson's ratio = 0.3 .
Ø16mm longitudinal bar and Ø6mm (longitudinal bar and stirrups) plastic property are taken from experimental test according to (ASTM A615/A615M-16) test

Mechanical properties of steel reinforcement.

Nominal diameter [mm]	Measured Diameter [mm]	Area [mm^2]	Yield stress f_y [MPa]	Ultimate stress f_u [MPa]	Elongation [%]
6	5.5	23. 75	623.96	685.5	8.5
16	16	200.96	569.67	668.79	12.5

Table 2: steel reinforcement property [Jasim,et al. 2020]

* Steel plate defined as isotropic with plastic property only with young modulus = 200*10^6MPa and poisson's ratio = 0.3 .

* Concrete property
Fc' = 27 MPa avg. and poisson's ratio = 0.2

* Ultra High Performance Concrete (UHPC)
Defend as concrete isotropic type , UHPC exhibits nonlinear behavior in both tension and compression, as seen in Fig 17 .

Property	Average value
Cubical compressive strength (MPa)	151.4
Direct tensile strength (MPa)	8.7
Modulus of elasticity (GPa)	41.0

Table 3 : properties of UHPC [Bahraq, Ashraf Awadh, et al. 2019}

Table 4 :Plasticity UHPC in ABAQUS

Dilation Angle, (ψ)	Viscosity, (μ)	Eccentricity	Stress ratio, (f_{b0}/f_{c0})	K
36˚	0.0001	0.1	1.16	0.667

Table 5 :Tension Nayal & Rasheeds Model In ABAQUS

Yield Tensile Stress, σt	εt ck Cracking Strain		dt damage Para.	εt ck Cracking Strain
0	0		0	0
3.814385927	0		0	0
2.937077164	3.16596E-05		0.23	3.16596E-05
1.716473667	0.000234149		0.55	0.000234149
0.1	0.000657845		0.97378346	0.000657845

3-2-3 Assembly the Model Parts

After modeling the elements and defining the materials, we group the elements together as we add the elements in the 3D field (independent) .

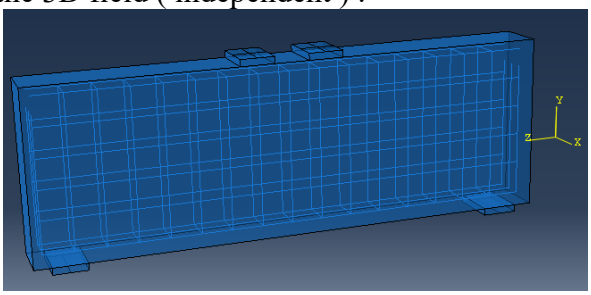

Figure 15: Assemble DP-S1 control beam

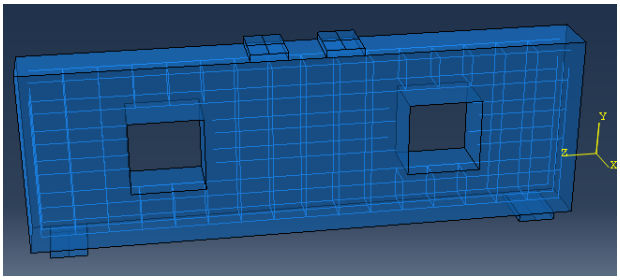

Figure 16 :Assemble DP-S1-C-O1

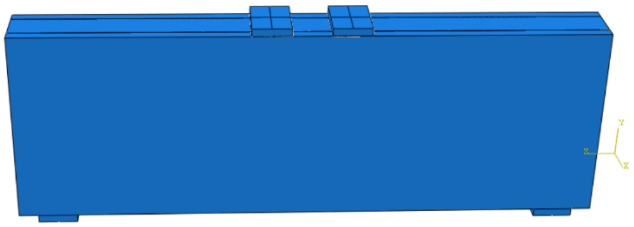

Figure 17:Assemble DP-S1-F-30

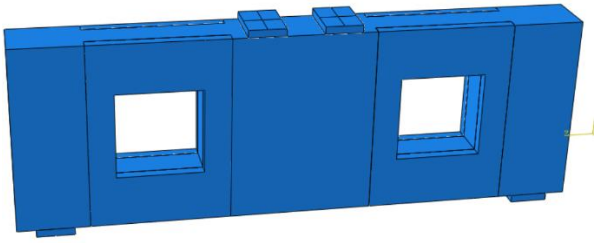

Figure 18: DP-S1-C-O2-G-30

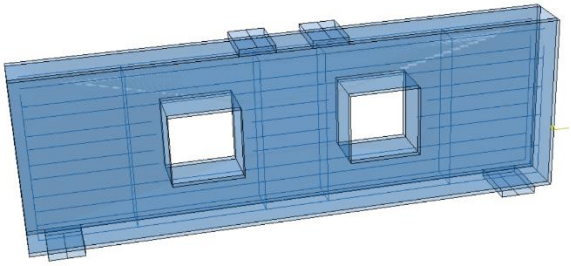

Figure 19:DP-S1-E-O1-SH-30

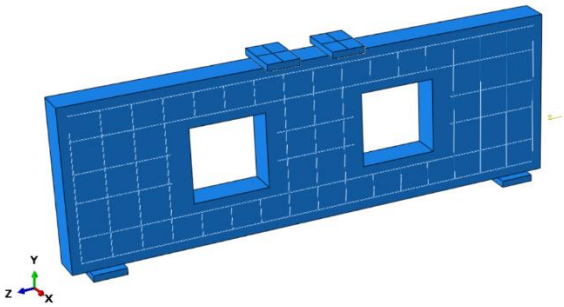

Figure 20 : Groved 30 mm "DP-S1-E-O2-F-30"

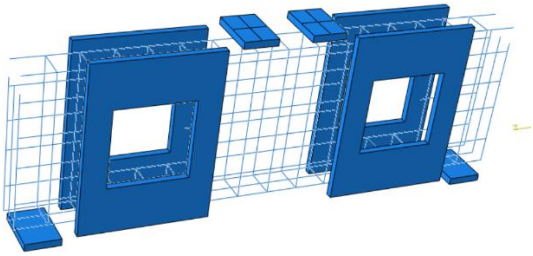

Figure 21 : UHPC with steel bars

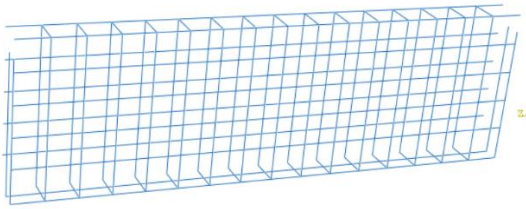

Figure 22 : Full steel bar and shear without opening

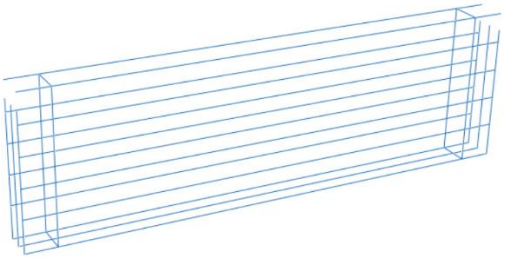

Figure 23 : steel bar without shear for deep beam without opening

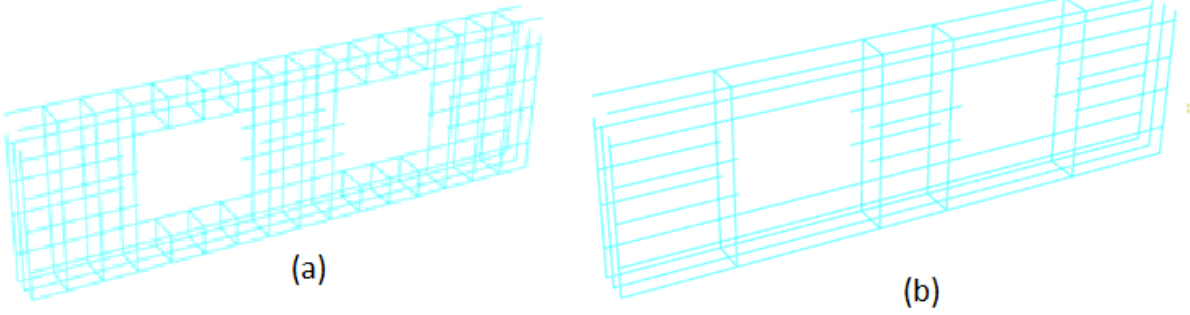

Figure 24 : (a)Full steel bar with opening ,(b) No shear full face strenght UHPC

3-2-4 Interaction

At this stage, bonding is made between the different elements, and there are several types of constrain according to the type of elements we use two type tie and embedded constrain . Tie constraint use to make bonding between solid (volume) element like concrete , UHPC , support and load plate . It is a bonding between surfaces of the elements so that they become a single mass that moves and affected together.

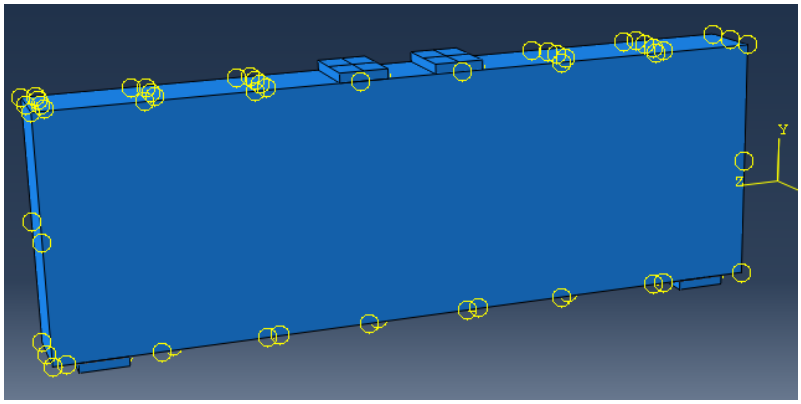

Figure 25 : Tie constrain between deep beam and support plate , deep beam and load plate

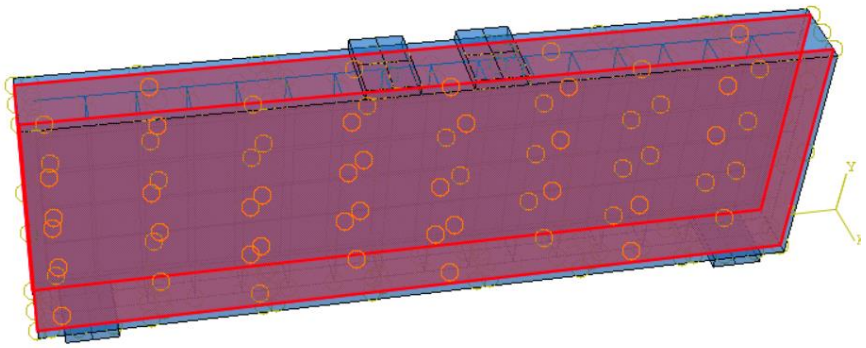

Figure 26:Tie constrain between deep beam and UHPC without opening

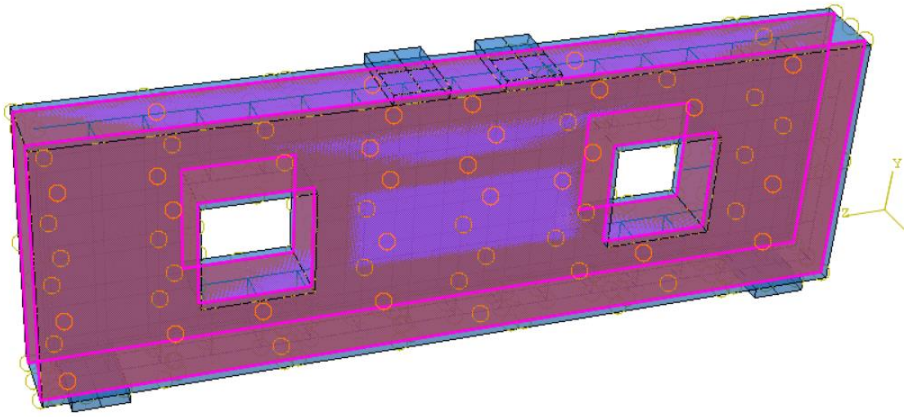

Figure 27:Tie constrain between deep beam and UHPC with opening

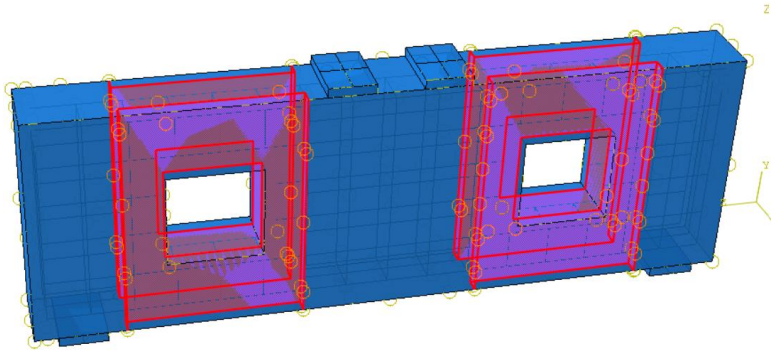

Figure 28 :Tie constrain between deep beam and grove layer of UHPC with opening

Embedded constraint : A collection of rebar-reinforced membrane, shell, or surface elements embedded in a set of three-dimensional solid components can be modeled using embedded constraint . truss or beam components inserted in a group of solid elements . This means that the internal elements are linked with the external element, move with it, and are affected by it . This type used to make a bonding between the wire - reinforced bar (longitudinal and stirrups) and the solid element - deep beam .

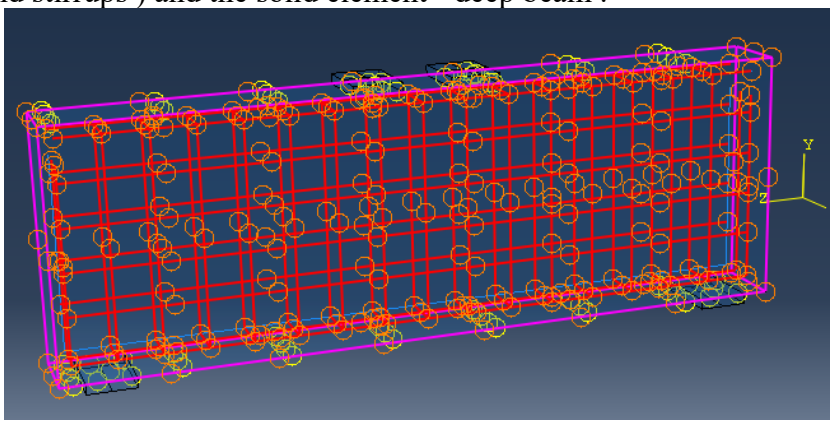

Figure 29 : embedded constrain between deep beam and steel reinforced

3-2-5 Boundary condition (BC's)

All deep beam modeled have roller support at right and pin support at left same as experimental test . In ABAQUS roller support only allowed vertical displacements to be restrained, while permitting rotations and longitudinal displacements . where pin support restraint to both vertical and longitudinal displacements (y and z direction) while allowing rotations about the (x – axis).

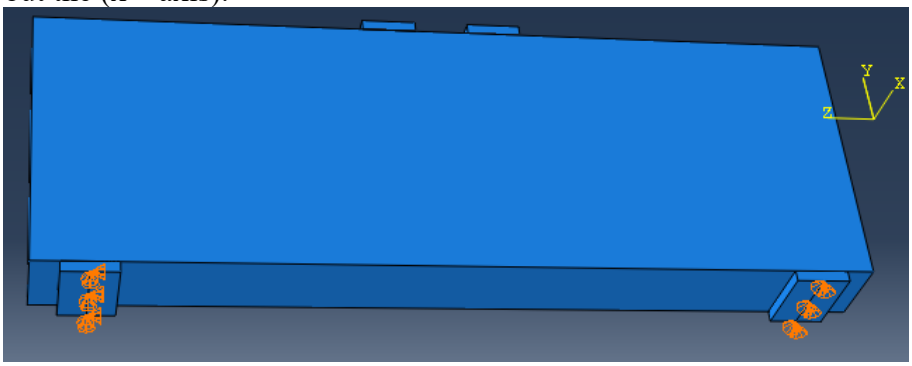

Figure 30 : boundary condition deep beam DP-S1

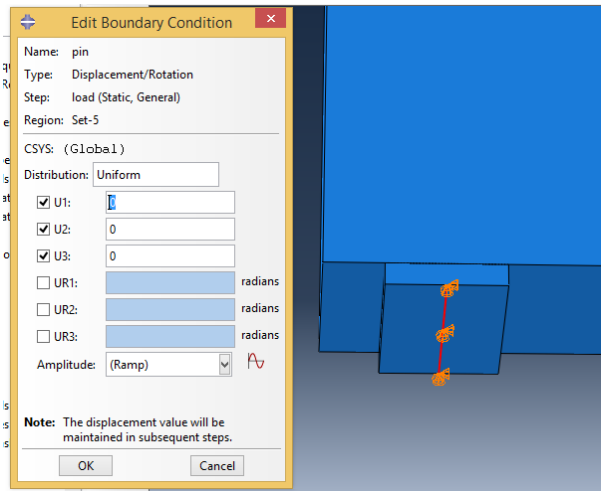

Figure 31 : BC's pin resistace ABAQUS

3-2-6 Load

Load defend as displacement force on both load plate ,so that there is a continuous load that increases until the beam reaches complete failure . (20mm displacement is used)

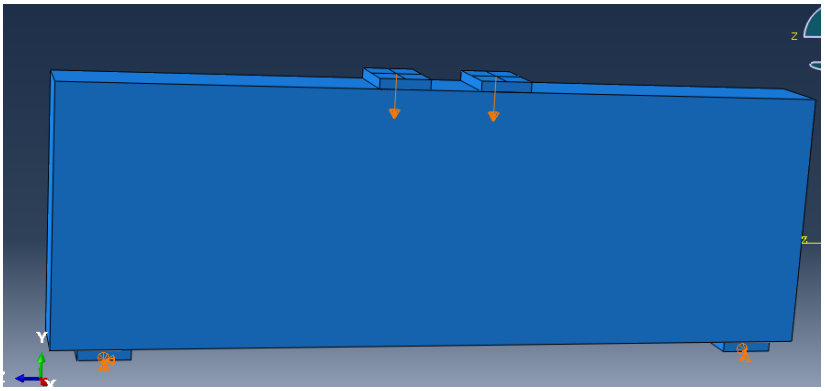
Figure 32 : displacement load on deep beam DP-S1

3-2-7 Meshing

It is the process of dividing the model into small parts, cubes, to facilitate the study of the effects on the element and to increase the accuracy of the outputs . mesh dimension adopted was 20*20 mm for all beam .

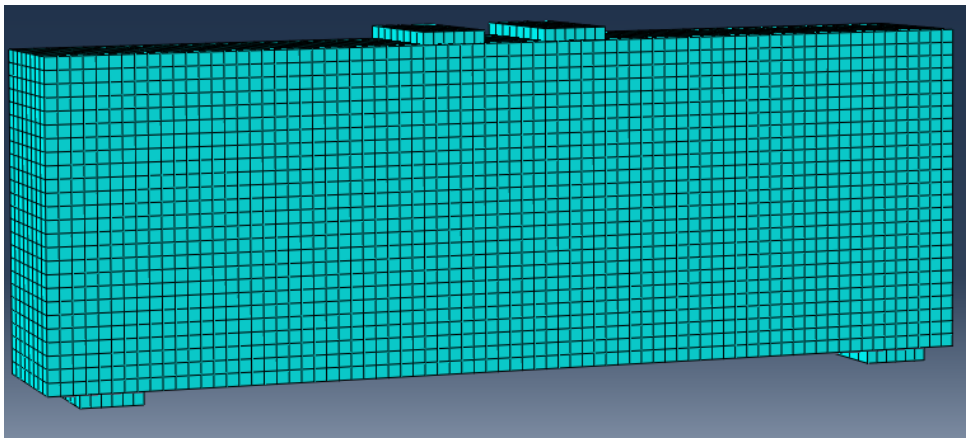

Figure 33 : meshing DP-S1

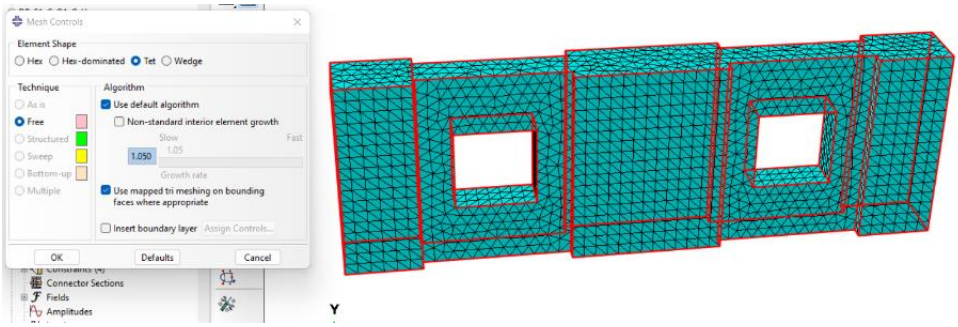

Figure 34:Tet Mesh for grove layer

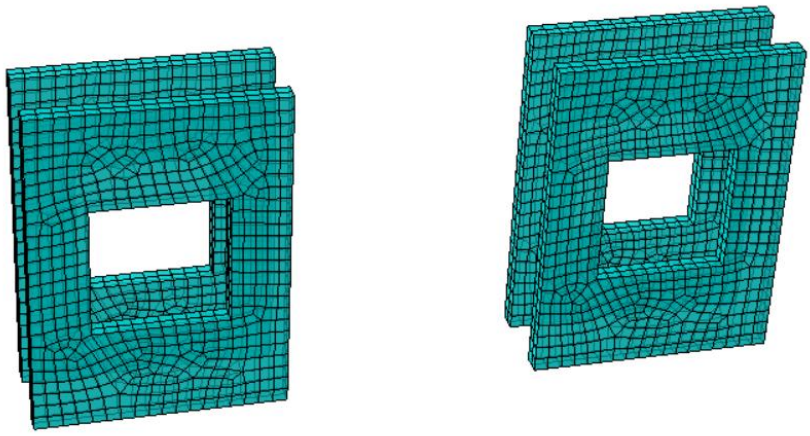

Figure 35: Mesh for UHPC layer

3-2-8 Job and visualization the model

After completing the samples processing we make a job for this sample and monitoring it , check there is no error and wait tell run is finish .

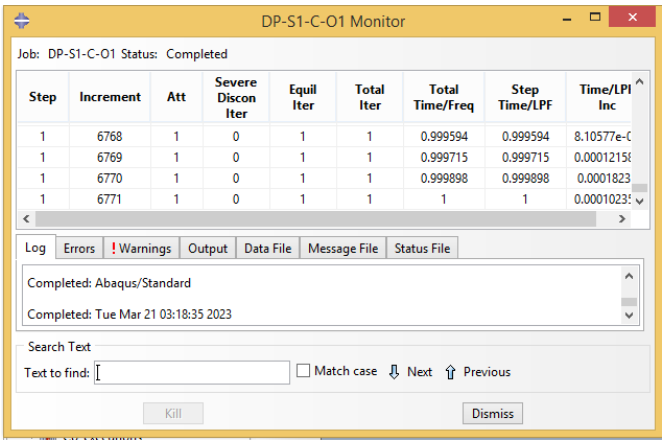

Figure 36 : job run for DP-S1-C-O1

The Visualization module displays finite element models and results graphically , deformed shape , damage compression , damage tension , …etc.

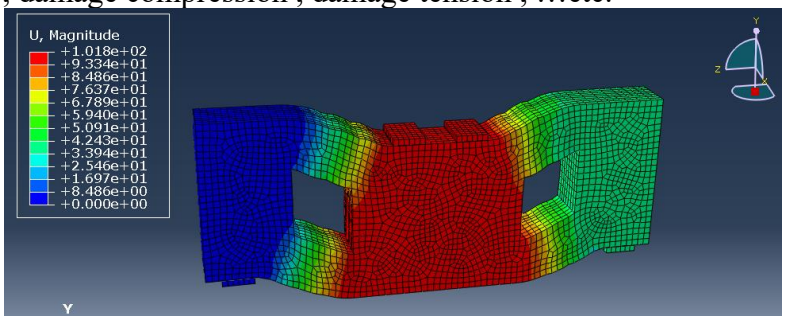

Figure 37 : Final deformed shape (U) for DP-S1-C-O1

3-3 Numerical Analysis Results

Table 6 :Verification between Experimental and ABAQUS result for control beam , First cracking load, failure load

Experimental(**EXP**)/ ABAQUS(**ABA**)	Specimen Designation	First Diagonal crack, (*kN*)	First diagonal crack, (%) (Experimental /ABAQUS)	First Flexural crack, (*kN*)	First flexural crack, (%) (Experimental /ABAQUS)	Failure load, (*kN*)	Failure load, (%)(Experimental/ ABAQUS)
EXP	DP-S1	120	-	135	-	500	-
ABA	DP-S1	107	1.12	121	1.11	479	104
EXP	DP-S1-C-O1	60	-	65	-	190	-
ABA	DP-S1-C-O1	63	0.95	81	0.80	199	0.95
EXP	DP-S1-C-O2	55	-	60	-	175	-
ABA	DP-S1-C-O2	47	1.17	65	0.92	162	1.08
EXP	DP-S1-E-O1	65	-	80	-	210	-
ABA	DP-S1-E-O1	61	1.07	74	1.13	206	1.02
EXP	DP-S1-E-O2	50	-	70	-	170	-
ABA	DP-S1-E-O2	55	0.91	76	0.92	179	0.95

Table 7 : Compase between ABAQUS result and parameter result for beam , First cracking load, failure load

BEAM #.	Specimen Designation	First Diagonal crack, (*kN*)	First diagonal crack, (%) (parameter /Control)	First Flexural crack, (*kN*)	First flexural crack, (%) (parameter /Control)	Failure load, (*kN*)	Failure load, (%)(parameter /Control)
1	DP-S1	107.00	-	121.00	-	479.00	-
2	DP-S1-F-30	203.00	1.90	229.00	1.89	660.00	1.38
3	DP-S1-F-SH-30	191.00	1.79	213.00	1.76	537.00	1.12
4	DP-S1-F-20	190.00	1.78	214.00	1.77	628.00	1.31
5	DP-S1-F-SH-20	184.00	1.72	207.00	1.71	487.00	1.02
6	DP-S1-C-O1	63.00	-	81.00	-	199.00	-
7	DP-S1-C-O1-F-30	68.00	1.08	82.00	1.01	282.00	1.42
8	DP-S1-C-O1-F-SH-30	53.00	0.84	78.00	0.96	237.00	1.19
9	DP-S1-C-O1-G-30	60.00	0.95	80.00	0.99	262.00	1.32
10	DP-S1-C-O1-G-SH-30	52.00	0.83	79.00	0.98	213.00	1.07
11	DP-S1-C-O1-F-20	53.00	0.84	80.00	0.99	249.00	1.25
12	DP-S1-C-O1-F-SH-20	42.00	0.67	68.00	0.84	175.00	0.88
13	DP-S1-C-O1-G-20	50.00	0.79	68.00	0.84	234.00	1.18
14	DP-S1-C-O1-G-SH-20	40.00	0.63	66.00	0.81	150.00	0.75
15	DP-S1-C-O2	47.00	-	65.00	-	162.00	-
16	DP-S1-C-O2-F-30	45.00	0.96	63.00	0.97	229.00	1.41
17	DP-S1-C-O2-F-SH-30	39.00	0.83	57.00	0.88	207.00	1.28

18	DP-S1-C-O2-G-30	40.00	0.85	57.00	0.88	224.00	1.38
19	DP-S1-C-O2-G-SH-30	31.00	0.66	48.00	0.74	143.00	0.88
20	DP-S1-C-O2-F-20	36.00	0.77	54.00	0.83	216.00	1.33
21	DP-S1-C-O2-F-SH-20	35.00	0.74	53.00	0.82	147.00	0.91
22	DP-S1-C-O2-G-20	38.00	0.81	56.00	0.86	199.00	1.23
23	DP-S1-C-O2-G-SH-20	30.00	0.64	45.00	0.69	130.00	0.70
24	DP-S1-E-O1	61.00	-	74.00	-	206.00	-
25	DP-S1-E-O1-F-30	74.00	1.21	117.00	1.58	302.00	1.47
26	DP-S1-E-O1-F-SH-30	46.00	0.75	105.00	1.42	234.00	1.14
27	DP-S1-E-O1-G-30	72.00	1.18	115.00	1.55	281.00	1.36
28	DP-S1-E-O1-G-SH-30	59.00	0.97	100.00	1.35	173.00	0.84
29	DP-S1-E-O1-F-20	71.00	1.16	113.00	1.53	282.00	1.37
30	DP-S1-E-O1-F-SH-20	60.00	0.98	105.00	1.42	174.00	0.84
31	DP-S1-E-O1-G-20	57.00	0.93	110.00	1.49	249.00	1.21
32	DP-S1-E-O1-G-SH-20	52.00	0.85	105.00	1.42	156.00	0.76
33	DP-S1-E-O2	55.00	-	76.00	-	179.00	-
34	DP-S1-E-O2-F-30	93.00	1.69	135.00	1.78	240.00	1.34
35	DP-S1-E-O2-F-SH-30	88.00	1.60	127.00	1.67	197.00	1.10
36	DP-S1-E-O2-G-30	84.00	1.53	120.00	1.58	232.00	1.30
37	DP-S1-E-O2-G-SH-30	80.00	1.45	108.00	1.42	201.00	1.12
38	DP-S1-E-O2-F-20	86.00	1.56	127.00	1.67	223.00	1.25
39	DP-S1-E-O2-F-SH-20	86.00	1.56	125.00	1.64	162.00	0.91
40	DP-S1-E-O2-G-20	84.00	1.53	125.00	1.64	202.00	1.13
41	DP-S1-E-O2-G-SH-20	79.00	1.44	103.00	1.36	165.00	0.92

Finite element model for DP-S1 “control beam”

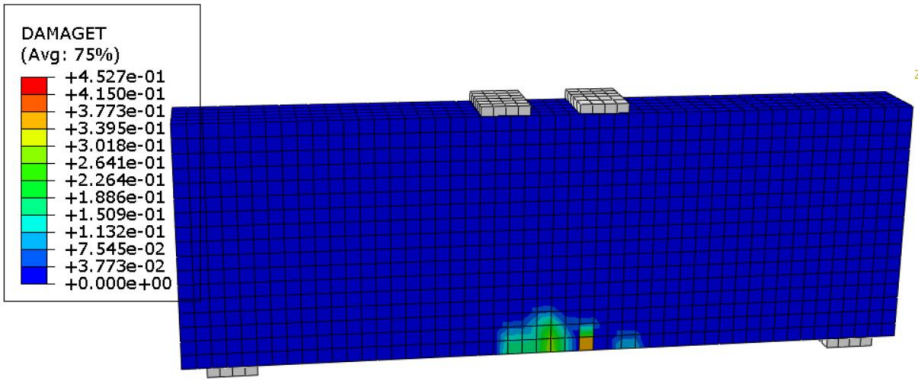

Figure 38 : First shear crack DP-S1

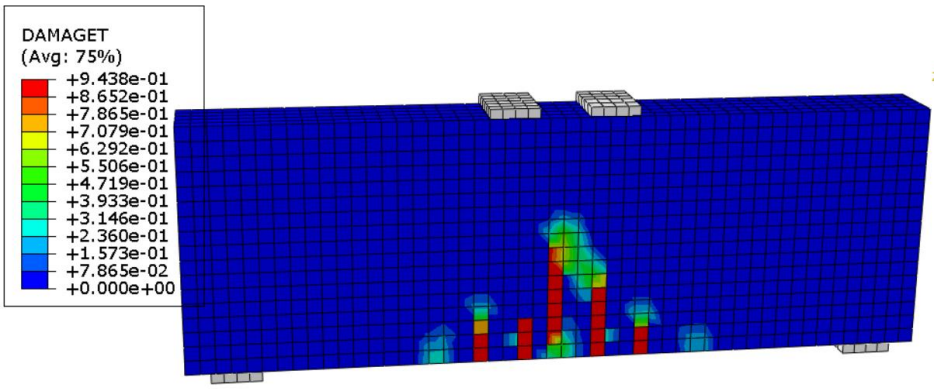

Figure 39 : First flexure crack DP-S1

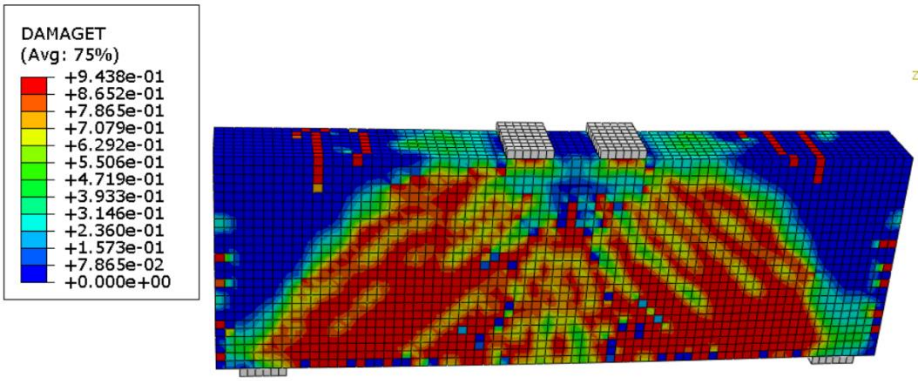

Figure 40 :Ultimate load crack at faiuler DP-S1 at 479.1KN&8.05mm

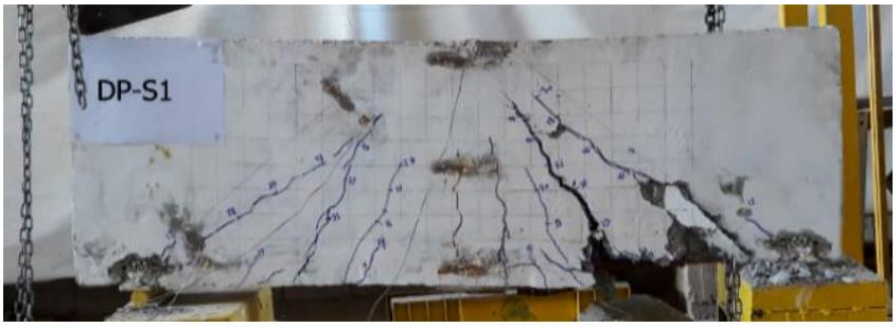

Figure 41 : Diagonal splitting failure of (DP-S1)

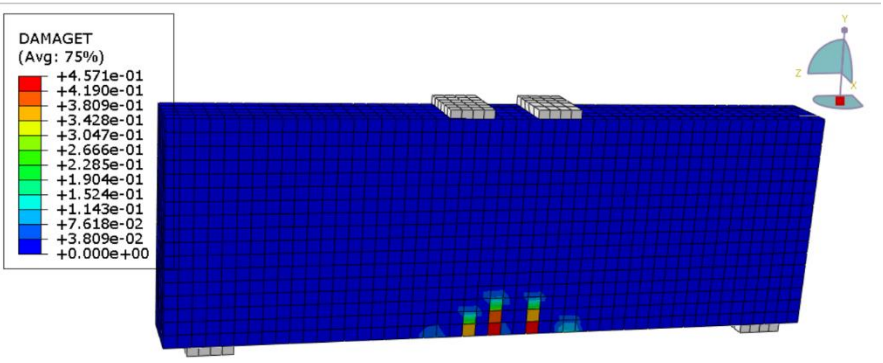

Figure 42 :First shear crack DP-S1-F-30

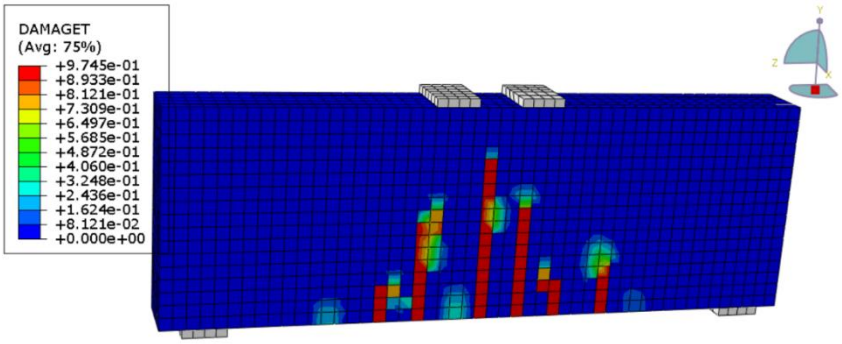

Figure 43 : First flexure crack DP-S1-F-30

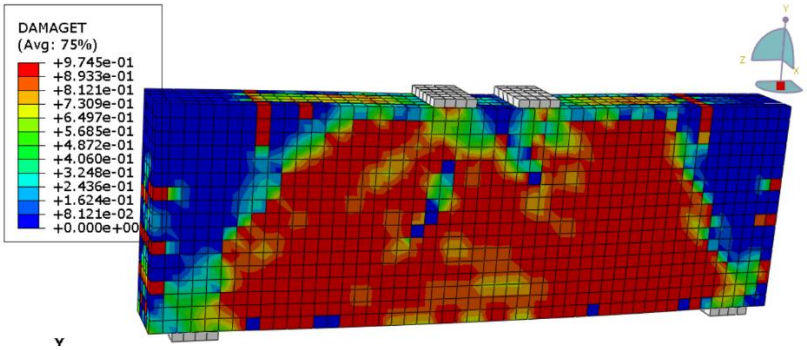

Figure 44 :Ultimate load crack at faiuler DP-S1-F-30

Finite element model for DP-S1-C-O1

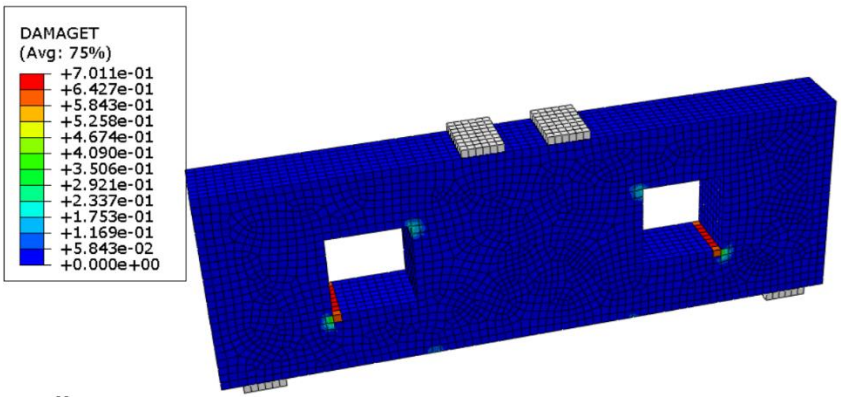

Figure 45:First shear crack DP-S1-C-O1

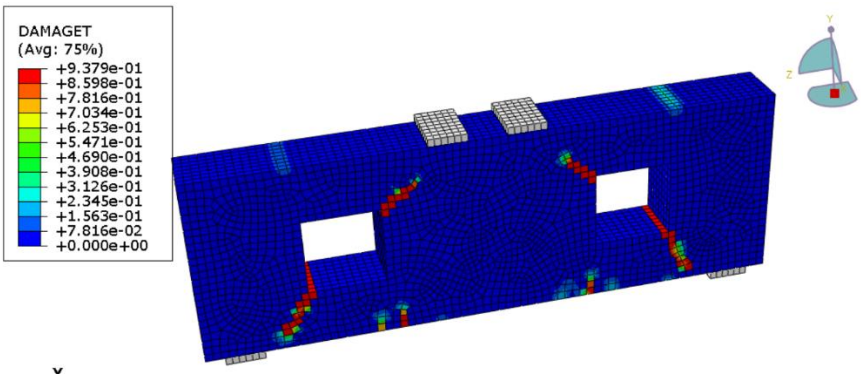

Figure 46 :First flexure crack DP-S1-C-O1

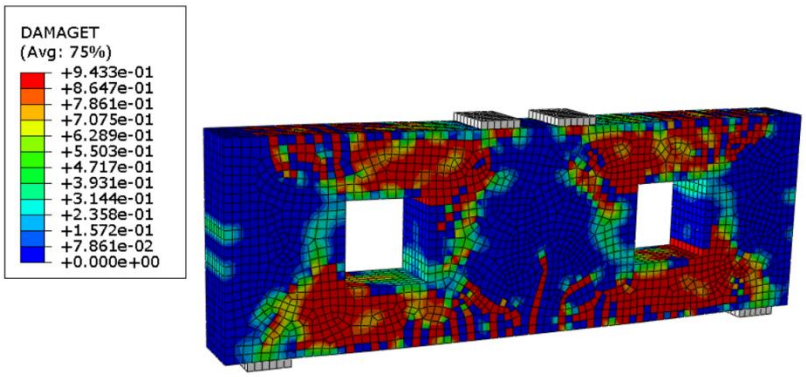

Figure 47 :Ultimate load crack at faiuler DP-S1-C-O1

Figure 48 : Diagonal splitting failure of DP-S1-C-O1 Expermintal

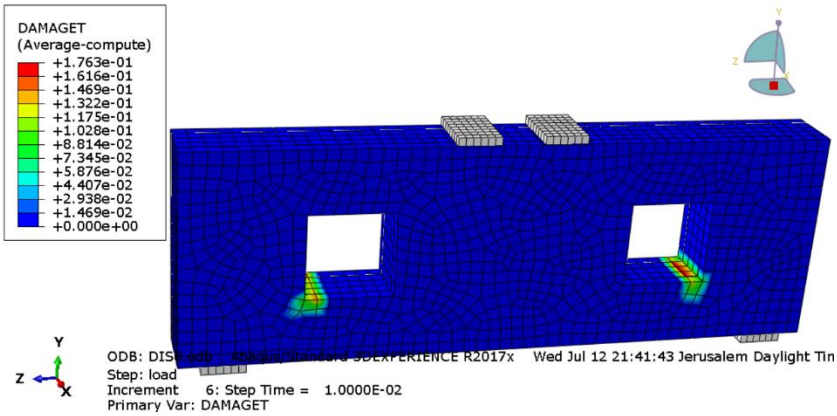

Figure 49 :First shear crack DP-S1-C-O1-F-30

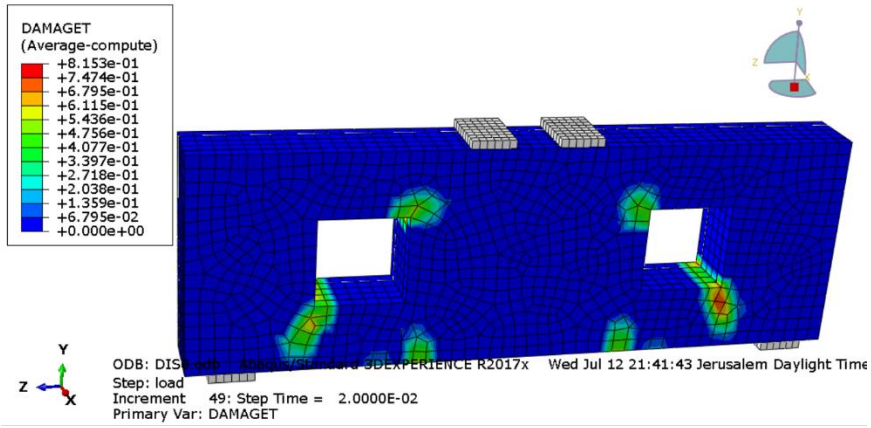

Figure 50 : First flexure crack DP-S1-C-O1-F-30

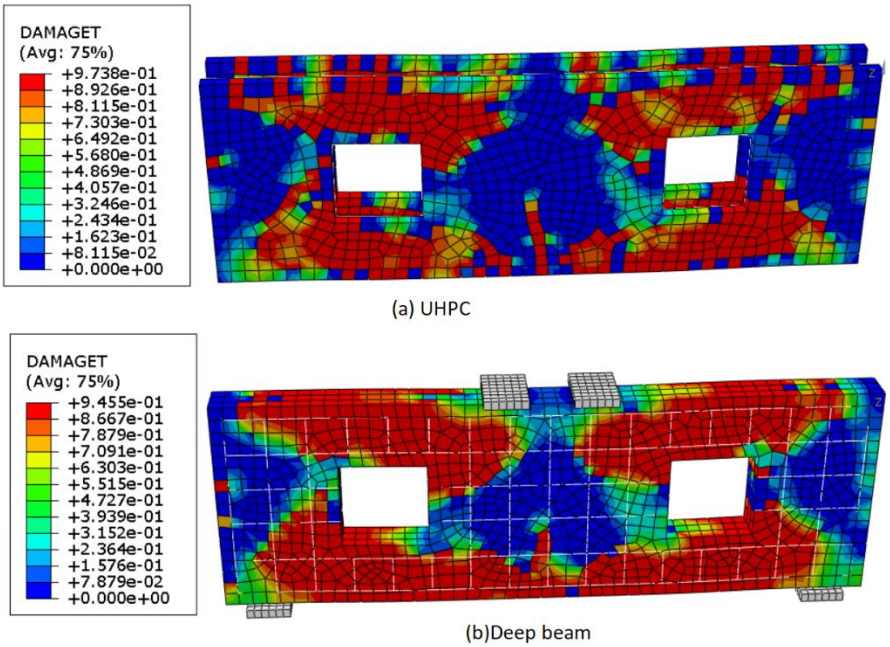

Figure 51 : Ultimate load crack at faiuler DP-S1-C-O1-F-30 (a)for UHPC 30mm full grove face , (b)deep beam

Table 8 : Verification between Experimental and ABAQUS result for control beam Deflection

Experimental(**EXP**)/ ABAQUS(**ABA**)	Specimen Designation	**Deflection, (mm)**	**Deflection**, (%) (Experimental /ABAQUS)
EXP	DP-S1	9	-
ABA	DP-S1	8.1	1.11
EXP	DP-S1-C-O1	4	-
ABA	DP-S1-C-O1	4.49	0.89
EXP	DP-S1-C-O2	4.3	-
ABA	DP-S1-C-O2	4.47	0.95
EXP	DP-S1-E-O1	4.8	-
ABA	DP-S1-E-O1	4.25	1.13
EXP	DP-S1-E-O2	5.1	-
ABA	DP-S1-E-O2	5.1	0.00

Table 9 : ABAQUS deflection mm for all deep beam with parameter

BEAM #.	Specimen Designation	**Deflection, (mm)**	**Deflection,** (%)(control/ parameter)
1	DP-S1	8.1	-
2	DP-S1-F-30	6.5	0.80
3	DP-S1-F-SH-30	3.1	0.38
4	DP-S1-F-20	5.9	0.73
5	DP-S1-F-SH-20	3.0	0.37

6	DP-S1-C-O1	4.49	-
7	DP-S1-C-O1-F-30	6.4	1.43
8	DP-S1-C-O1-F-SH-30	3.6	0.80
9	DP-S1-C-O1-G-30	5.2	1.16
10	DP-S1-C-O1-G-SH-30	3.2	0.71
11	DP-S1-C-O1-F-20	5.97	1.33
12	DP-S1-C-O1-F-SH-20	2.96	0.66
13	DP-S1-C-O1-G-20	5.94	1.32
14	DP-S1-C-O1-G-SH-20	3.0	0.67
15	DP-S1-C-O2	4.46	-
16	DP-S1-C-O2-F-30	8.1	1.82
17	DP-S1-C-O2-F-SH-30	5.08	1.14
18	DP-S1-C-O2-G-30	5.95	1.33
19	DP-S1-C-O2-G-SH-30	3.5	0.78
20	DP-S1-C-O2-F-20	7.14	1.60
21	DP-S1-C-O2-F-SH-20	3.56	0.80
22	DP-S1-C-O2-G-20	4.19	0.94
23	DP-S1-C-O2-G-SH-20	2.85	0.64
24	DP-S1-E-O1	4.25	-
25	DP-S1-E-O1-F-30	6.1	1.44
26	DP-S1-E-O1-F-SH-30	5.34	1.26
27	DP-S1-E-O1-G-30	5.06	1.19
28	DP-S1-E-O1-G-SH-30	4.17	0.98
29	DP-S1-E-O1-F-20	5.61	1.32
30	DP-S1-E-O1-F-SH-20	5.08	1.20
31	DP-S1-E-O1-G-20	5.06	1.19
32	DP-S1-E-O1-G-SH-20	2.85	0.67
33	DP-S1-E-O2	5.1	-
34	DP-S1-E-O2-F-30	7.16	1.40
35	DP-S1-E-O2-F-SH-30	5.17	1.01

36	DP-S1-E-O2-G-30	5.87	1.15
37	DP-S1-E-O2-G-SH-30	5.11	1.00
38	DP-S1-E-O2-F-20	7.11	1.39
39	DP-S1-E-O2-F-SH-20	5.66	1.11
40	DP-S1-E-O2-G-20	4.16	0.82
41	DP-S1-E-O2-G-SH-20	5.74	1.13

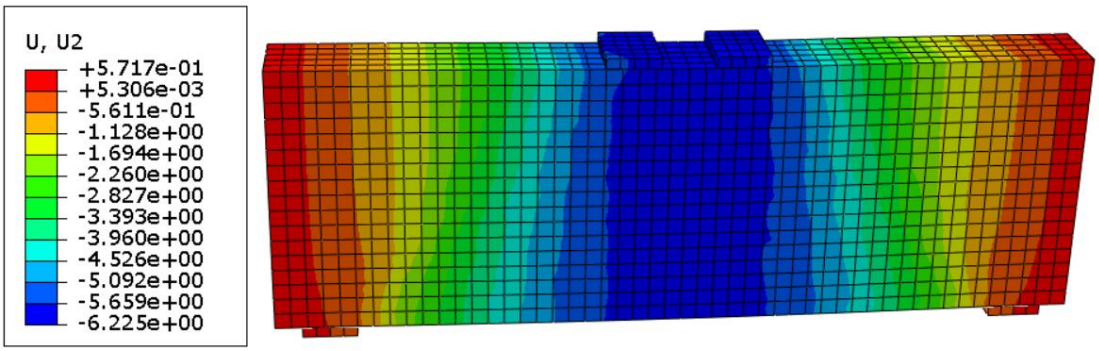

Figure 52 : Deflection for (DP-S1)

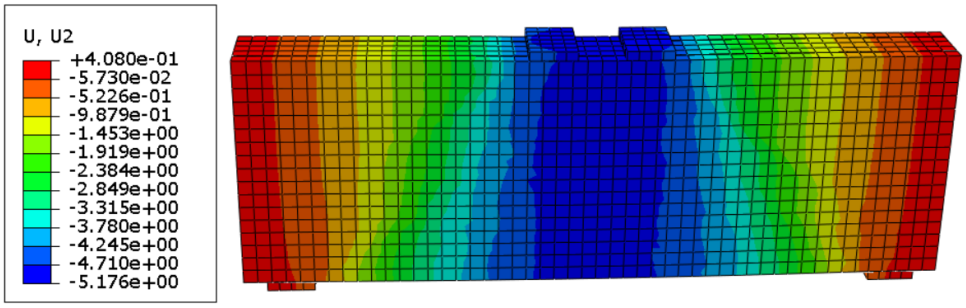

Figure 53 : Deflection for (DP-S1-F-30)

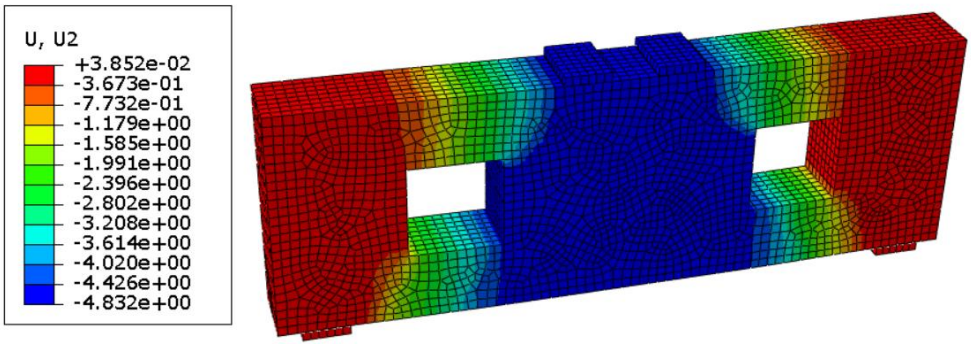

Figure 54 : Deflection for (DP-S1-C-O1)

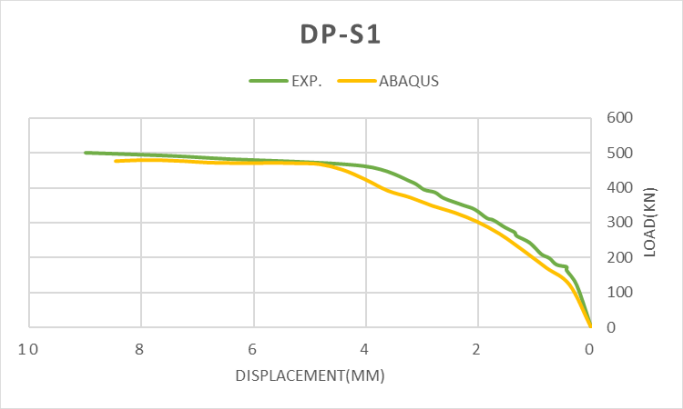

Figure 55 : Load – Displacement Curve for DP-S1 copmerssion between experimental and ABAQUS

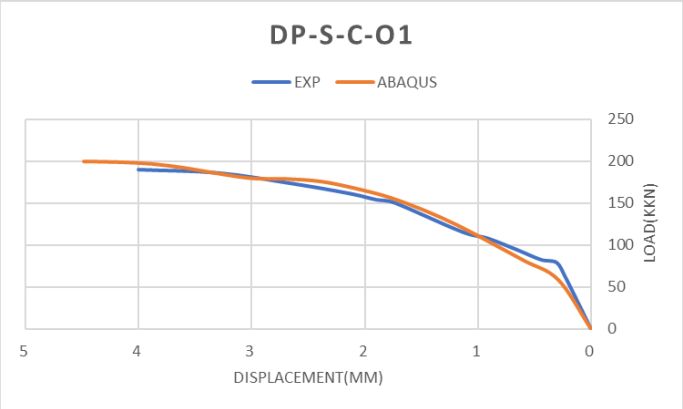

Figure 56 : Load – Displacement Curve for DP-S1-C-O1 copmerssion between experimental and ABAQUS

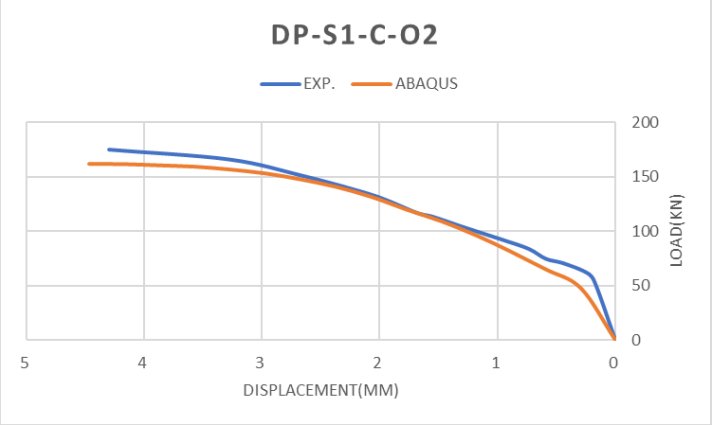

Figure 57 : Load – Displacement Curve for DP-S1-C-O2 copmerssion between experimental and ABAQUS

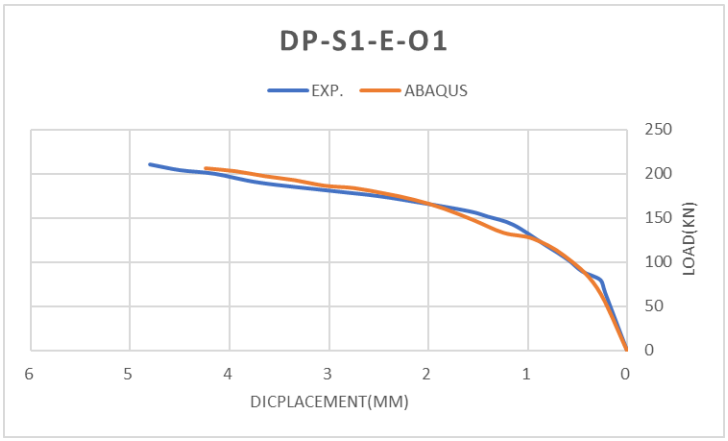

Figure 58 : Load – Displacement Curve for DP-S1-E-O1 copmerssion between experimental and ABAQUS

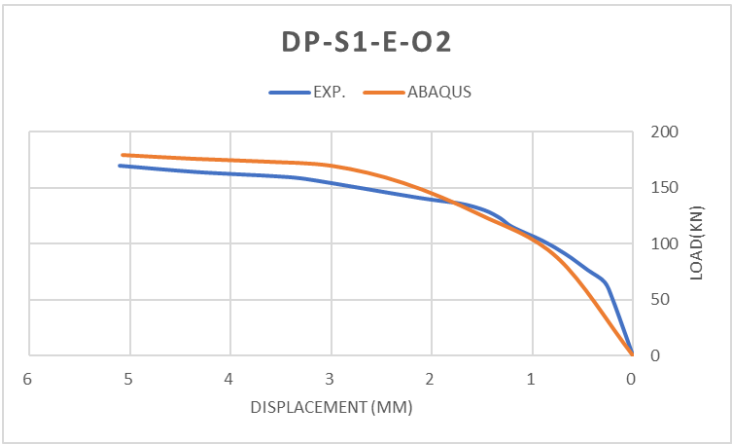

Figure 59 : Load – Displacement Curve for DP-S1-E-O2 copmerssion between experimental and ABAQUS

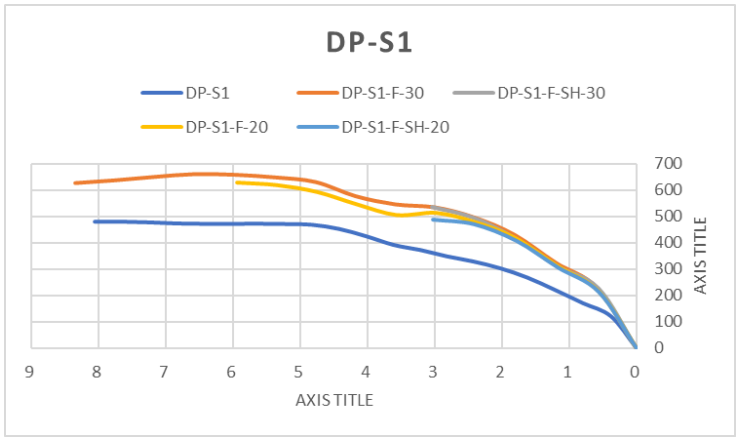

Figure 60 : Load displacement curve for DP-S1 with parameter

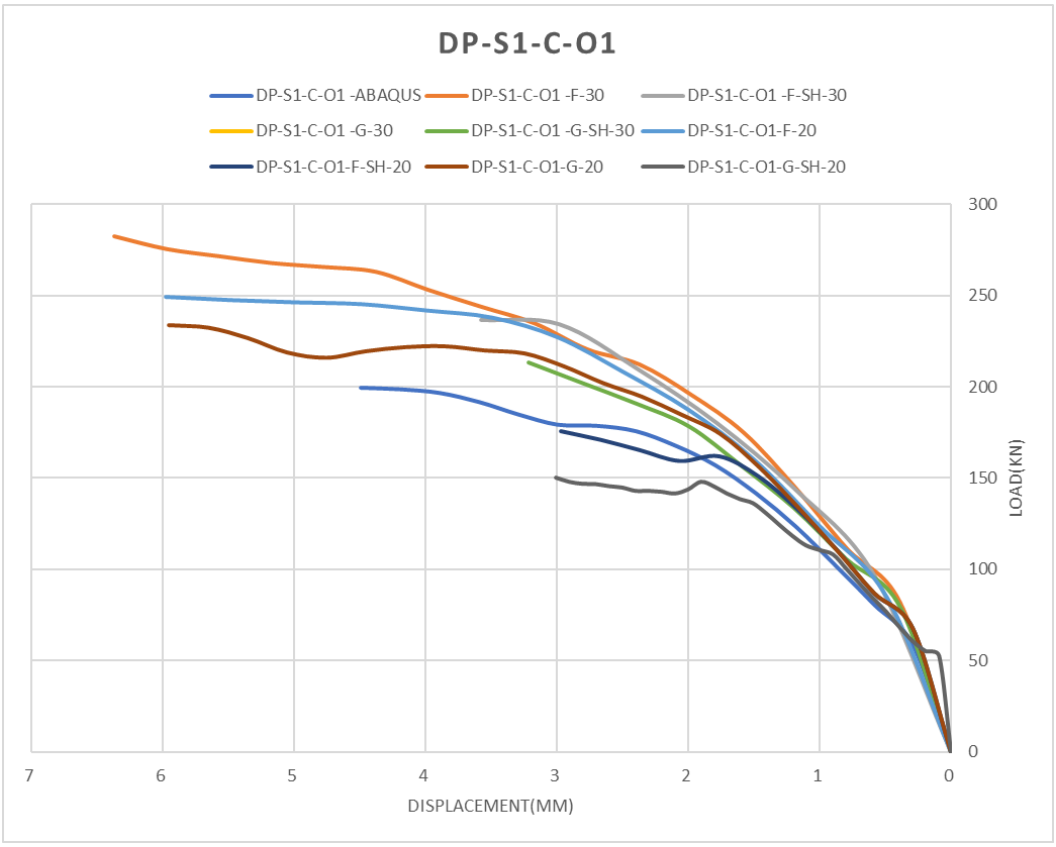

Figure 61 : Load displacement curve for DP-S1-C-O1 with parameter

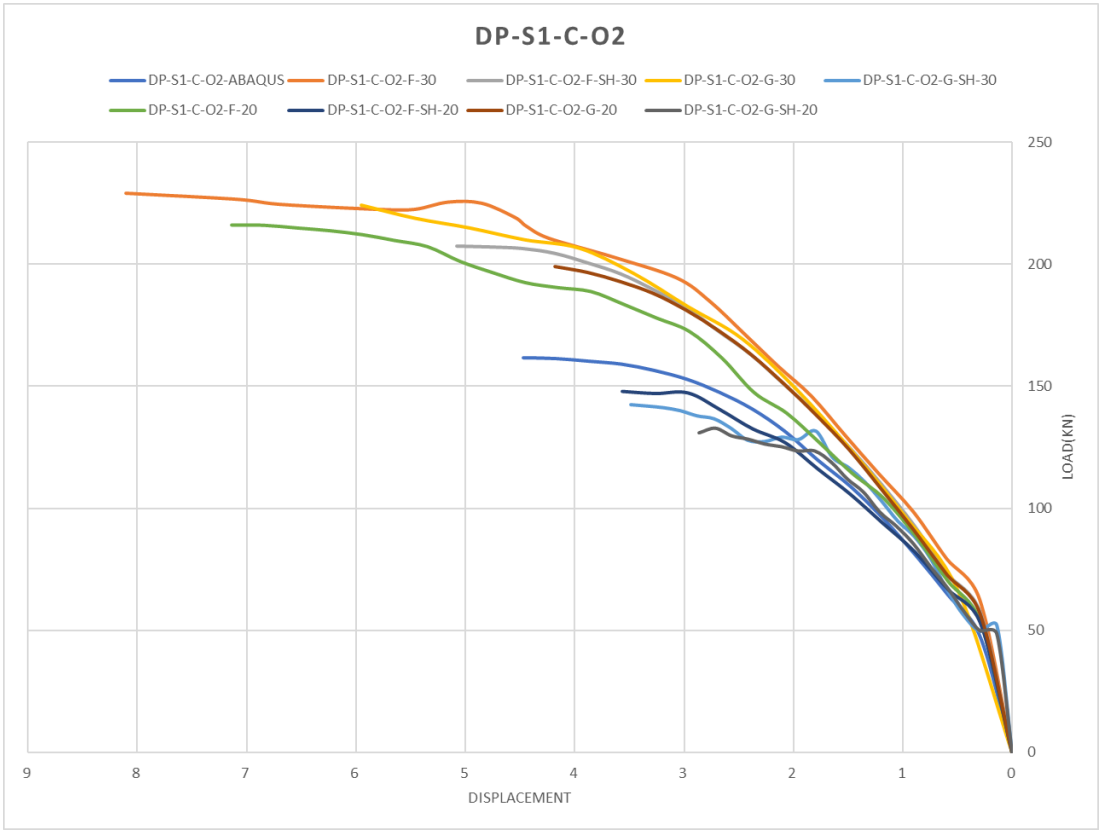

Figure 62 : Load displacement curve for DP-S1-C-O2 with parameter

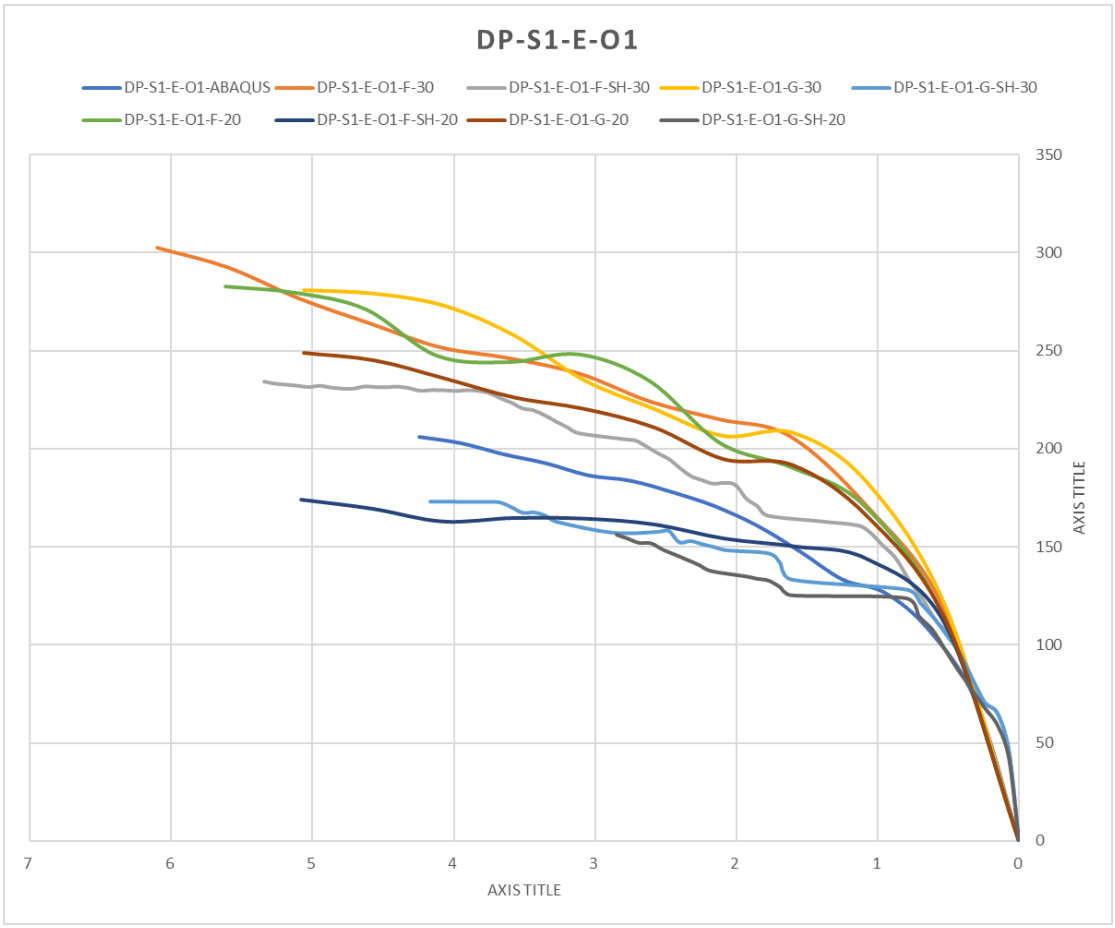

Figure 63 : Load displacement curve for DP-S1-E-O1 with parameter

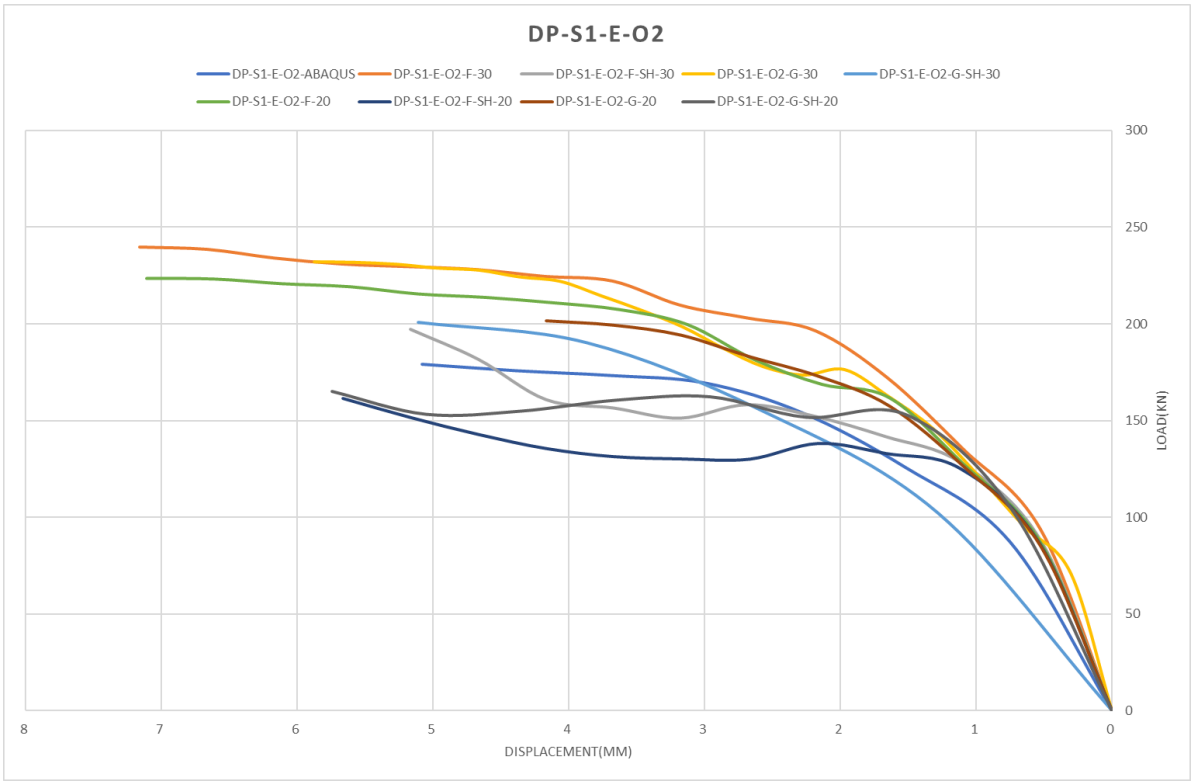

Figure 64 : Load displacement curve for DP-S1-E-O2 with parameter

Chapter 4: STRUT AND TIE

4-1 GENERAL

In this chapter, the Strut and tie (STM) method will be studied . Due to the different characteristics of deep beam from ordinary beam, as mentioned previously (not following Bernoulli's theory), other methods were necessary to analyze and understand the behavior of these elements, and the most prominent of these methods is the strut and tie method (STM). The strut and tie model is a viable approach, although it introduces considerable uncertainty because to the numerous models that may be utilized. This method was used in some studies as a model for the distribution of reinforced steel .

4-2 Description of the Issue

For developing structures made of cracked reinforced concrete, the strut and tie model is regarded as an intelligent and reliable foundation. Several recent advances of design equations based on truss models have pushed the benefits to the side. The issue is that elastic stress analysis may be a superior design than STM if optimal modeling is not used.

4-3 Elements of Strut and Tie Model

A structural truss, as seen in Figure 9, is used to describe the strut and tie model in deep beams. The members and components of this model are as follows:

1- Strut: Compressive force resisted by concrete, In Figure 9, The Strut provides as the diagonal compression component between the load and support zones, and it is compressed when the load passes through it and hits the support.

2-Tie: is the tension member in strut and tie model. In Figure 9, They are made out of a combination of reinforcement and concrete. The contribution of concrete to the tensile resistance of a tie is neglected. However, the presence of concrete helps to improve stiffness and control deformations

3- Nodal Zone: The intersection between the axes of two or more struts and ties . These are confined areas of concrete that should satisfy strength requirements. These nodes, which serve as the truss model's joints, may be classified into four groups based on how the truss model was created:

1- C-C-C node resists three compressive forces.
2- C-C-T node resists two compressive forces and one tensile force.
3- C-T-T node resists one compressive force and two tensile forces.

The classification of nodes are shown in Figure 10.

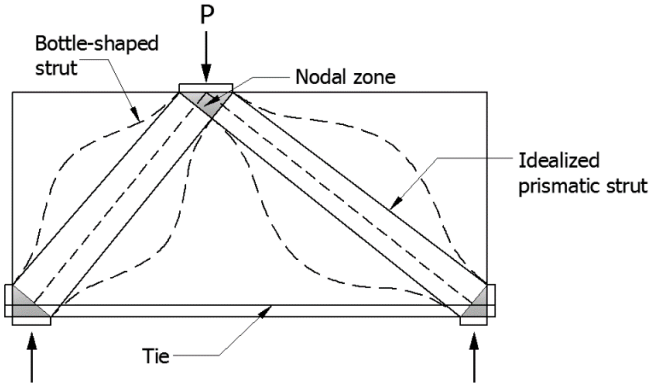

Figure 65: strut and tie model in deep beam

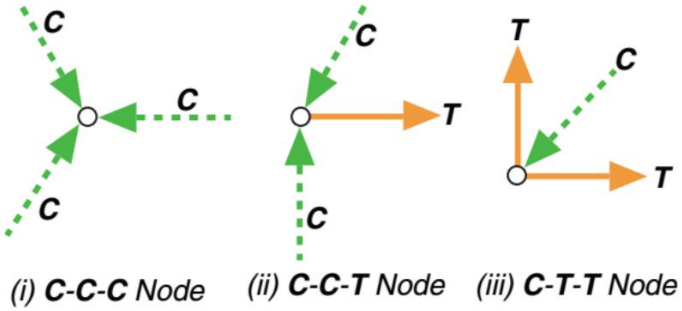

Figure 66:type of node in strut and tie model

Forces follow the shortest possible path moving loads , strut and tie must be design according to this theory . The strut and tie lines are drawn through the crack lines in the element or through the tension and compression areas resulting from the finite element model .

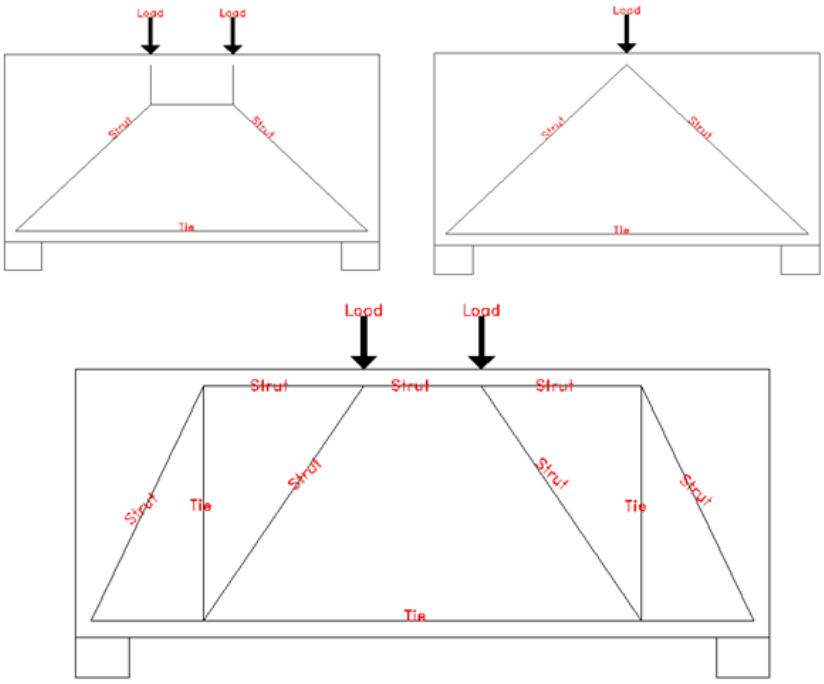

Figure 67:Possible load paths for deep without opening

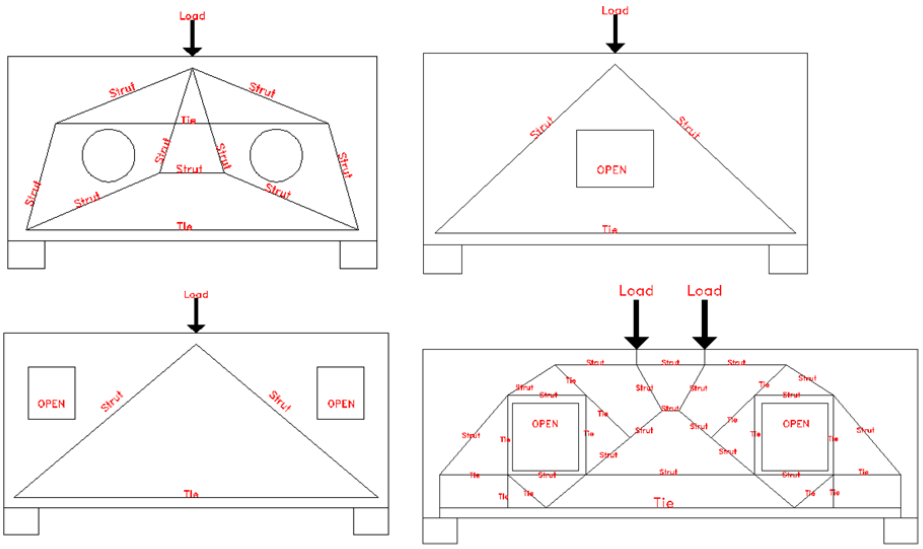

Figure 68 :Possible load paths for deep with opening

4-5 Solution mechanism

AStrutTie2017 program is using to solve and draw the strut and tie developed by HANGIL IT CO.,LTD .

4-5-1 Strength of struts

The nominal compressive strength of a strut without longitudinal reinforcement, Fns, must be interpreted in accordance with ACI 318-14 .

$$F_{ns} = f_{ce}^{s} A_{cs}$$ Equation 1

where f_{ce}^{s} is the smaller of:

- The effective compressive strength of the concrete in the strut.
- The effective compressive strength of the concrete in the nodal zone.

and A_{cs} is the cross-sectional area at one end of the strut. In calculating A_{cs}, the strut width is measured perpendicular to the strut axis at its end.

The effective compressive strength of the concrete in a strut fce can be obtained from

$$f_{ce}^{s} = 0.85 f_c' \beta_s$$ Equation 2

where βs is a concrete efficiency factor and fc ′ is the concrete cylinder strength. According to the ACI 318-14 Code, Table 10 displays the values of βs, which indicate how the stress conditions, strut shape, and the angle of cracking around the strut affect strength.

Table 10 : ACI 318-14 code values of coefficient βs

Strut condition	β_s
• A strut with constant cross-section along its length	1.0
• For struts located such that the width of the midsection of the strut is larger than the width at the nodes (bottle-shaped struts)	
a) With reinforcement normal to strut center-line to resist the transverse tension	0.75
b) Without reinforcement normal to the center-line of the strut	0.6λ
• For struts in tension members, or the tension flanges of members	0.40
• For all other cases	0.6λ

The following equation can be used to determine the concrete's effective compressive strength, or fce:

$$f_{ce}^{n} = 0.85 f_c' \beta_n$$ Equation 3

Where βn is a nodal zone's efficacy factor. The effectiveness factor, n, for nodal zones in accordance with the ACI 318-14 Code is shown in Table 11.

4-5-2Reinforced ties

The notional strength of a tie, Fnt, is defined as Fnt = Astfy, where Ast denotes the steel area and fy the yield stress. To ensure node safety, the width of a tie must be set, with an upper limit of wt,max.

wt = 0.0

If only one row of bars is used, and enough development length is provided beyond the nodal zones over a distance of at least 2c, where c is the concrete cover,

$wt = \emptyset bar + 2c$ Equation 4

Where $\boldsymbol{\emptyset bar}$ is the diameter of the reinforcing bars

If more than one row of bars is used, it must be possible to extend the development length beyond the nodal zones by at least s/2, where s is the clear distance between the bars.

wt = n$\emptyset bar$ + 2c + (n – 1)s

Where n is the number of rows of reinforcing bars

The intersection of the centroid of the tie's bars and the extensions of either the strut's or the bearing area's shape marks the start of the development length according to ACI 318-14, $lanc$

$$w_{t,max} = \frac{F_{nt}}{b\, f_{ce}^{n}}$$ Equation 5

Table 11 : ACI 318-14 Code values of coefficient βn for nodes

Nodal zone	β_n
For nodal zones bounded by struts or bearing areas or both, C-C-C node	1.00
Nodal zones anchoring one tie, C-C-T node	0.80
Nodal zones anchoring two or more ties with the presence of one strut, C-T-T node	0.60
Nodal zones anchoring ties only, T-T-T node	0.40

4-6 Design Conditions (AStrutTie Program result)
4-6-1 DP-S1

* Project Name : DP-S1
* Design Code : ACI 318M-14
* Unit : KN.m
* Strength Reduction Factors
  Strut : 0.75 , Tie : 0.75 , Node : 0.75

4-6-1-2 Strut-Tie Model Design (Load Combination-1)

Construction of Strut-Tie Model

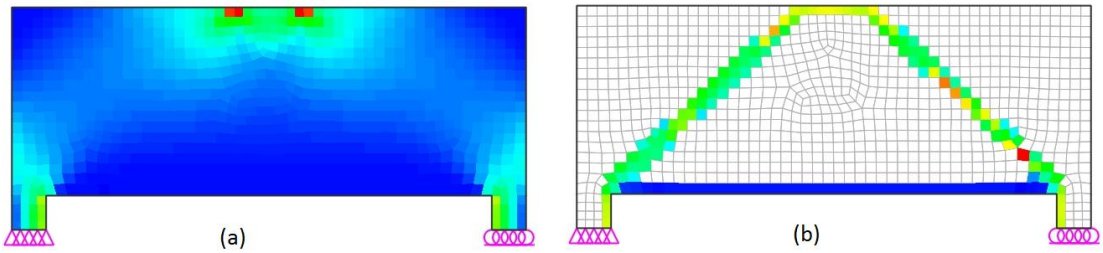

Figure 69 : ESO (Evolutionary Structural Optimization) (a)STAGE-01 (Initial shape) , (b) STAGE-20 (Elimination ratio = 84%)

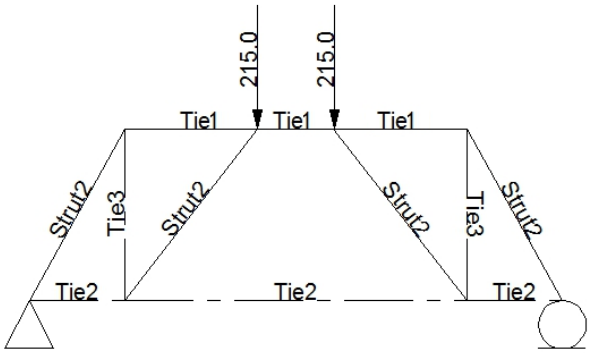

Figure 70 : Strut and Tie type

- Strut1 : Prismatic Strut
- Strut2 : Bottle Shape Strut (Satisfying ACI 318M-14 23.5.3)
- Tie1 : Tie for top rebars
- Tie2 : Tie for bottom rebars
- Tie3 : Tie for intermediate vertical/horizontal rebars

4-6-1-3 Strut and Tie Forces

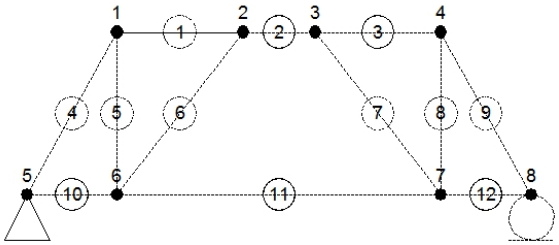

Figure 71 : truss element and node number

Table 12 : truss element force

Elem. No.	Force (kN)	Elem. No.	Force (kN)	Elem. No.	Force (kN)	Elem. No.	Force (kN)
1	-119.4	2	-286.7	3	-119.4	4	-246.0
5	215.0	6	-272.4	7	-272.4	8	215.0
9	-246.0	10	119.4	11	286.7	12	119.4

4-6-1-4 Strength Verification and Required Rebars

Strength under Bearing/Loading Plates

phi fce = phi·0.85·beta·fck < Fu / A

beta = 1.00 (for the nodal zone bounded by struts, bearing areas, or both)

0.80 (for the nodal zone anchoring one tie)

0.60 (for the nodal zone anchoring two or more ties)

A = Area of bearing plates (= BxW)

Node	beta	fce(MPa)	Fu (kN)	B (mm)	W (mm)	Fu/A (MPa)	Note
5	0.80	12.24	215.0	150.0	100.0	14.333	O.K
8	0.80	12.24	215.0	150.0	100.0	14.333	O.K
2	1.00	15.30	215.0	150.0	100.0	14.333	O.K
3	1.00	15.30	215.0	150.0	100.0	14.333	O.K

4-6-1-5 Required Area of Rebars

Available Widths of Struts and Nodal Zones

1) Node without bearing plate

The available widths of a strut at both ends and nodal zone faces are determined by taking the minimum ones from the values calculated below for case 1 and case 2.

2) Node with bearing plate

The available widths of a strut at both ends and nodal zone faces are determined by taking the values calculated below for case 3.

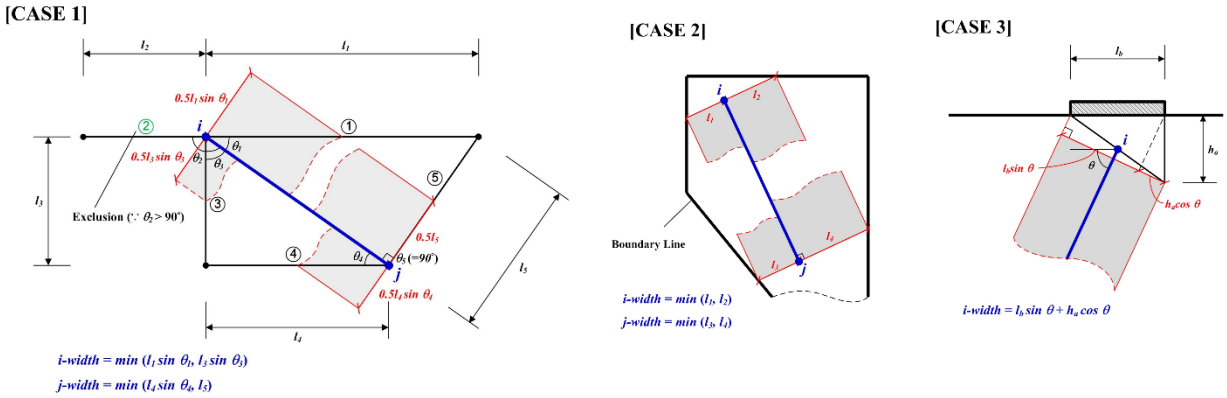

The available widths of struts and ties determined by the methods introduced above are shown below

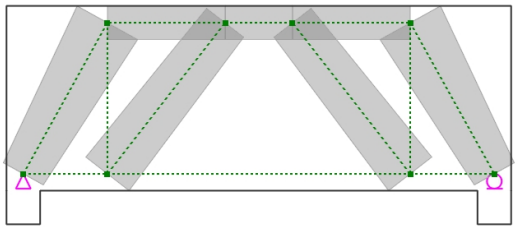

Figure 72 :available widths of struts and ties

4-6-1-6 Strength of Nodal Zones

The verification of the nodal zone strength should be done through comparing the available nodal zone area with that required. In this report, if the thickness of the structural concrete is consistent, the verification will be done by comparing the available nodal zone width, Wprov, with that required, Wreq

Wreq = Fu / phi·0.85·beta·fck·b < Wprov (See ACI 318M-14 Section 23.9)

beta = 1.00 (for the nodal zone bounded by struts, bearing areas, or both)

0.80 (for the nodal zone anchoring one tie)

0.60 (for the nodal zone anchoring two or more ties)

1) Concentrated Node

(A) Node 2 (CCC)

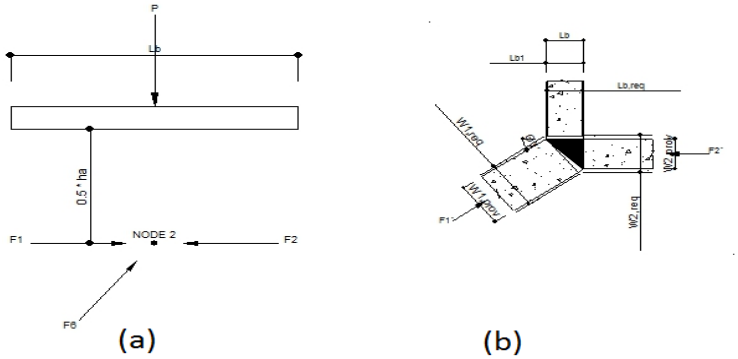

Lb = 100.0 mm , ha = 100.0 mm , P = 215.00 kN

Lb1 = P1/P×Lb = [F1×sin(theta 1)+F6×sin(theta 6)]/P×Lb

= [119.44×sin(0.0)+272.38×sin(52.1)]/215.00×100.0= 100.0 mm

F1′ = sqrt{[F1×cos(theta 1)+F6×cos(theta 6)]²+ [F1×sin(theta 1)+F6×sin(theta 6)]²}

= sqrt{[119.44×cos(0.0)+272.38×cos(52.1)]²+ [119.44×sin(0.0)+272.38×sin(52.1)]²} = 358.33 kN

theta 1′ = atan([F1×sin(theta 1)+F6×sin(theta 6)]/ [F1×cos(theta 1)+F6×cos(theta 6)])

= atan([119.44×sin(0.0)+272.38×sin(52.1)]/ [119.44×cos(0.0)+272.38×cos(52.1)]) = 36.9 deg.

Lb2 = P2/P×Lb = [F2×sin(theta 2)]/P×Lb = [286.67×sin(0.0)]/215.00×100.0 = 0.0 mm

F2′ = sqrt{[F2×cos(theta 2)]²+ [F2×sin(theta 2)]²} = sqrt{[286.67×cos(0.0)]²+ [286.67×sin(0.0)]²} = 286.67 kN

theta 2′ = atan([F2×sin(theta 2)]/[F2×cos(theta 2)]) = atan([286.67×sin(0.0)]/ [286.67×cos(0.0)]) = 0.0 deg.

W1,prov = Lb1×sin(theta 1′)+ha×cos(theta 1′)= 100.00×sin(36.9)+100.00×cos(36.9) = 140.0 mm

W2,prov = Lb2×sin(theta 2′)+ha×cos(theta 2′)= 100.00×sin(0.0)+100.00×cos(0.0) = 140.0 mm

W1,req = F1′/[phi×0.85×beta×fck×b] = (358.33×1000)/[0.75×0.85×1.00×30.0×150.00]

= 124.91 mm > W1,prov = 140.0 mm (OK)

W2,req = F2′/[phi×0.85×beta×fck×b] = (286.67×1000)/[0.75×0.85×1.00×30.0×150.00]

= 99.90 mm > W2,prov = 100.0 mm (OK)

Lb,req = P/[phi×0.85×beta×fck×b] = (215.00×1000)/[0.75×0.85×1.00×24.0×150.00]

= 93.7 mm = Lb,req = 100.0 mm (OK)

(B) Node 3 (CCC)

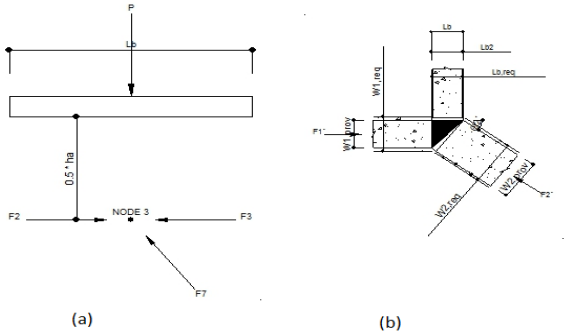

Lb1 = P1/P×Lb = [F2×sin(theta 2)]/P×Lb= [286.67×sin(0.0)]/215.00×100.0= 0.0 mm

F1′ = sqrt{[F2×cos(theta 2)]²+ [F2×sin(theta 2)]²} = sqrt{[286.67×cos(0.0)]²+ [286.67×sin(0.0)]²} = 286.67 kN

theta 1′ = atan([F2×sin(theta 2)]/ [F2×cos(theta 2)]) = atan([286.67×sin(0.0)]/ [286.67×cos(0.0)])

= 0.0 deg.

Lb2 = P2/P×Lb = [F3×sin(theta 3)+F7×sin(theta 7)]/P×Lb

= [119.44×sin(0.0)+272.38×sin(52.1)]/215.00×100.0= 100.0 mm

F2′ = sqrt{[F3×cos(theta 3)+F7×cos(theta 7)]²+ [F3×sin(theta 3)+F7×sin(theta 7)]²}

= sqrt{[119.44×cos(0.0)+272.38×cos(52.1)]²+ [119.44×sin(0.0)+272.38×sin(52.1)]²}

= 358.33 kN

theta 2′ = atan([F3×sin(theta 3)+F7×sin(theta 7)]/ [F3×cos(theta 3)+F7×cos(theta 7)])

= atan([119.44×sin(0.0)+272.38×sin(52.1)]/ [119.44×cos(0.0)+272.38×cos(52.1)])

= 36.9 deg.

W1,prov = Lb1×sin(theta 1′)+ha×cos(theta 1′)= 0.00×sin(0.0)+100.00×cos(0.0) = 100.0

W2,prov = Lb2×sin(theta 2′)+ha×cos(theta 2′)= 100.00×sin(36.9)+100.00×cos(36.9) = 140.0

W1,req = F1′/[phi×0.85×beta×fck×b] = (286.67×1000)/[0.75×0.85×1.00×30×150.00]

= 99.9 mm > W1,prov = 100.0 mm (OK)

W2,req = F2′/[phi×0.85×beta×fck×b] = (358.33×1000)/[0.75×0.85×1.00×30×150.00]

= 124.9 mm > W2,prov = 140.0 mm (OK)

Lb,req = P/[phi×0.85×beta×fck×b] = (215.00×1000)/[0.75×0.85×1.00×24.0×150.00]

= 93.7 mm = Lb,req = 100.0 mm (OK)

(C) Node 5 (CCT)

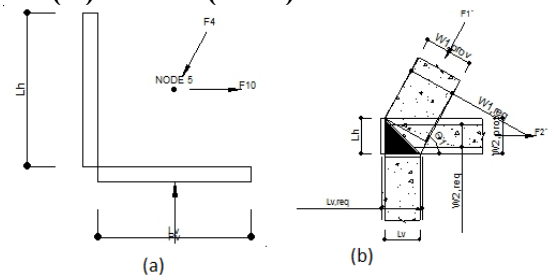

F1′ = sqrt{[F4×cos(theta 4)]²+ [F4×sin(theta 4)]²}

= sqrt{[245.95×cos(60.9)]²+ [245.95×sin(60.9)]²} = 245.95 kN

theta 1′ = atan([F4×sin(theta 4)]/ [F4×cos(theta 4)])

= atan([245.95×sin(60.9)]/ [245.95×cos(60.9)]) = 60.9 deg.

F2′ = F10= 119.44 kN

theta 2′ = theta 10 = 0.0 deg.

W1,prov = Lv×sin(theta 1′)+Lh×cos(theta 1′)= 100.00×sin(60.9)+100.00×cos(60.9) = 136.0 mm

W2,prov = Lv×sin(theta 2′)+Lh×cos(theta 2′)= 100.00×sin(0.0)+100.00×cos(0.0) = 100.0 mm

W1,req = F1′/[phi×0.85×beta×fck×b] = (245.95×1000)/[0.75×0.85×0.80×30×150.00]

= 134.0 mm = W1,prov = 136.0 mm (OK)

W2,req = F2′/[phi×0.85×beta×fck×b] = (119.44×1000)/[0.75×0.85×0.80×24.0×150.00]

= 65.1 mm = W2,prov = 100.0 mm (OK)

Lv,req = Pv/[phi×0.85×beta×fck×b] = (215.00×1000)/[0.75×0.85×0.80×20×150.00]

= 117.1 mm > Lv,req = 100.0 mm (OK)

(D) Node 8 (CCT)

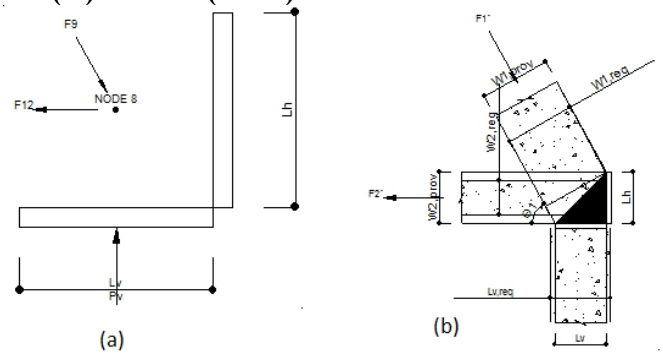

F1′ = sqrt{[F9×cos(theta 9)]²+ [F9×sin(theta 9)]²}

= sqrt{[245.95×cos(60.9)]²+ [245.95×sin(60.9)]²} = 245.95 kN

theta 1′ = atan([F9×sin(theta 9)]/ [F9×cos(theta 9)])

= atan([245.95×sin(60.9)]/ [245.95×cos(60.9)]) = 60.9 deg.

F2′ = F12 = 119.44 kN

theta 2′ = theta 12 = 0.0 deg.

W1,prov = Lv×sin(theta 1′)+Lh×cos(theta 1′)= 100.00×sin(60.9)+100.00×cos(60.9)= 136.0 mm

W2,prov = Lv×sin(theta 2′)+Lh×cos(theta 2′)= 100.00×sin(0.0)+100.00×cos(0.0) = 100.0 mm

W1,req = F1′/[phi×0.85×beta×fck×b] = (245.95×1000)/[0.75×0.85×0.80×24.0×150.00]
= 134.0 mm = W1,prov = 136.0 mm (OK)
W2,req = F2′/[phi×0.85×beta×fck×b] = (119.44×1000)/[0.75×0.85×0.80×30.0×150.00]
= 65.1 mm = W2,prov = 100.0 mm (OK)
Lv,req = Pv/[phi×0.85×beta×fck×b] = (215.00×1000)/[0.75×0.85×0.80×30.0×150.00]
= 74.9 mm < Lv,req = 100.0 mm (OK)

Pn	215	kN
2Pn (P_{STM})	430	kN
P_{ABAQUS}	479	kN
P_{STM} / P_{ABAQUS}	0.897	

Failure occurred due to the yielding of the tension ties.

4-6-2 DP-S1-F-30

4-6-1-2 Construction of Strut-Tie Model

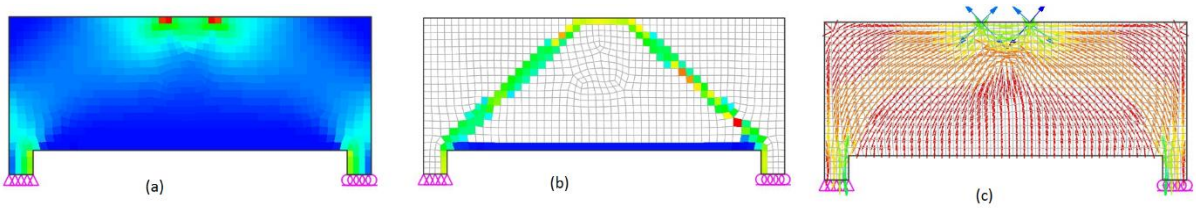

Figure 73 : (a) STAGE-01 (Initial shape),(b)STAGE-20 (Elimination ratio = 84%), (c) Compressive Principal Stress Flow.

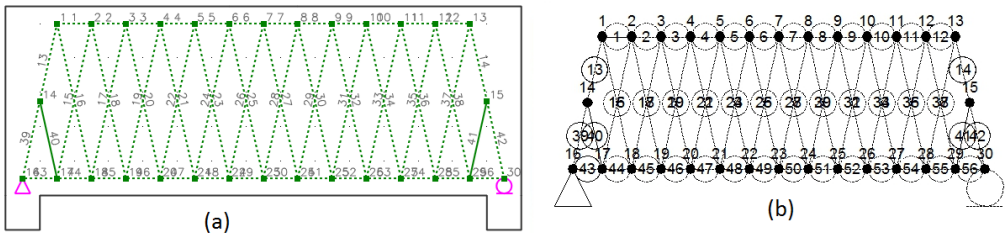

Figure 74 : (a) Constructed Strut-Tie Model , (b) Strut and Tie Forces

Table 13 : Strut and Tie Forces

Elem. No.	Force (kN)	Elem. No.	Force (kN)	Elem. No.	Force (kN)	Elem. No.	Force (kN)
1	-5.4	2	-74.7	3	-80.0	4	-149.3
5	-154.7	6	-186.2	7	-191.6	8	-147.5
9	-152.9	10	-71.1	11	-76.5	12	5.4
13	-12.4	14	12.4	15	-159.7	16	12.4
17	-12.4	18	159.7	19	-159.7	20	12.4
21	159.7	22	-12.4	23	12.4	24	-159.7
25	-14.5	26	-12.4	27	12.4	28	14.5

29	-12.4	30	-188.6	31	188.6	32	12.4
33	-12.4	34	-188.6	35	188.6	36	12.4
37	-12.4	38	-188.6	39	-161.3	40	-41.8
41	-41.8	42	-96.4	43	385.2	44	59.4
45	64.8	46	134.1	47	139.4	48	208.7
49	214.1	50	207.8	51	213.2	52	131.4
53	136.8	54	54.9	55	60.3	56	20.9

3) Strength Verification and Required Rebars

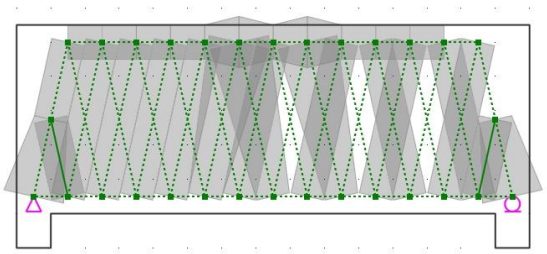

Figure 75 : Available Widths of Struts and Nodal Zones

Strength of Struts

Strut No.	beta	theta	Fu (kN)	b (mm)	Wreq (mm)	Wprov (mm)	Note
1	1.00	0.0	5.4	150.0	1.9	100.0	O.K
2	1.00	0.0	74.7	150.0	26.0	100.0	O.K
3	1.00	0.0	80.0	150.0	27.9	100.0	O.K
4	1.00	0.0	149.3	150.0	52.1	100.0	O.K
5	1.00	0.0	154.7	150.0	53.9	100.0	O.K
6	1.00	0.0	186.2	150.0	64.9	100.0	O.K
7	1.00	0.0	191.6	150.0	66.8	100.0	O.K
8	1.00	0.0	147.5	150.0	51.4	100.0	O.K
9	1.00	0.0	152.9	150.0	53.3	100.0	O.K
10	1.00	0.0	71.1	150.0	24.8	100.0	O.K
11	1.00	0.0	76.5	150.0	26.6	100.0	O.K
13	0.75	77.5	12.4	150.0	5.8	97.6	O.K
15	0.75	77.5	159.7	150.0	74.2	97.6	O.K
17	0.75	77.5	12.4	150.0	5.8	97.6	O.K
19	0.75	77.5	159.7	150.0	74.2	97.6	O.K
22	0.75	77.5	12.4	150.0	5.8	97.6	O.K
24	0.75	77.5	159.7	150.0	74.2	97.6	O.K
25	0.75	77.5	14.5	150.0	6.7	97.6	O.K
26	0.75	77.5	12.4	150.0	5.8	97.6	O.K

29	0.75	77.5	12.4	150.0	5.8	97.6	O.K
30	0.75	77.5	188.6	150.0	87.7	97.6	O.K
33	0.75	77.5	12.4	150.0	5.8	97.6	O.K
34	0.75	77.5	188.6	150.0	87.7	97.6	O.K
37	0.75	77.5	12.4	150.0	5.8	97.6	O.K
38	0.75	77.5	188.6	150.0	87.7	97.6	O.K
39	0.75	77.5	161.3	150.0	75.0	97.6	O.K
40	1.00	77.5	41.8	150.0	14.6	97.6	N.G
41	1.00	77.5	41.8	150.0	14.6	97.6	O.K
42	0.75	77.5	96.4	150.0	44.8	97.6	O.K

Node 6 (CCC)

F1′ = 415.08 kN

theta 1′ = 24.2 deg.

W1,req = 144.7 mm = W1,prov = 198.3 mm (OK)

Lh,req = 0.0 mm = Lh,req = 150.0 mm (OK)

Lv,req = 59.3 mm = Lv,req = 150.0 mm (OK)

(B) Node 8 (CCT)

F1′ = 422.27 kN , F2′ = F28 = 14.46 kN

theta 1′ = 25.8 deg. , theta 2′ = theta 28 = 77.5 deg.

W1,req = 184.0 mm = W1,prov = 200.4 mm (OK)

W2,req = 6.3 mm = W2,prov = 179.0 mm (OK)

Lh,req = 0.0 mm = Lh,req = 150.0 mm (OK)

Lv,req = 74.1 mm = Lv,req = 150.0 mm (OK)

(C) Node 16 (CCT)

F1′ = 161.29 kN , F2′ = F43= 385.21 kN

theta 1′ = 77.5 deg. , theta 2′ = theta 43= 0.0 deg.

W1,req = 70.3 mm = W1,prov = 179.0 mm (OK)

W2,req = 149.1 mm > W2,prov = 150.0 mm (OK)

Lh,req = 126.5 mm > Lh,req = 150.0 mm (OK)

Lv,req = 68.6 mm = Lv,req = 150.0 mm (OK)

(D) Node 30 (CCT)

F1′ = 96.43 kN , F2′ = F56 = 20.92 kN

theta 1′= 77.5 deg. , theta 2′ = theta 56 = 0.0 deg.

W1,req = 42.0 mm = W1,prov = 179.0 mm (OK)

W2,req = 9.1 mm = W2,prov = 150.0 mm (OK)

Lh,req = 0.0 mm = Lh,req = 150.0 mm (OK)

Lv,req = 41.0 mm = Lv,req = 150.0 mm (OK)

Pn	305	kN
2Pn (P_{STM})	610	kN
P_{ABAQUS}	660	kN
P_{STM} / P_{ABAQUS}	0.924	

Failure occurred due to the yielding of the tension ties

4-6-3 DP-S1-C-O1

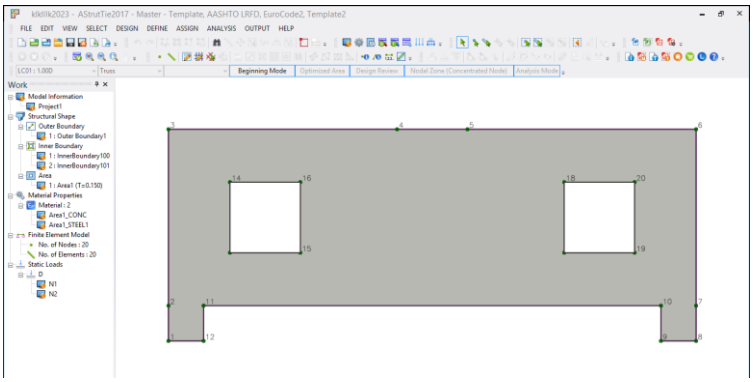

Figure 76 : DP-S1-C-O1 AStrutTie program

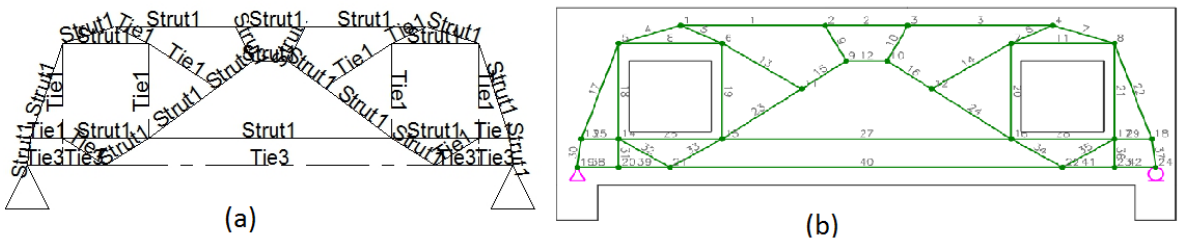

Figure 77 : (a)strut and tie in DP-S1-C-O1 , (b) element and nod number

- Strut1 : Prismatic Strut
- Tie1 : Tie for vertical/horizontal rebars
- Tie3 : Tie for intermediate bottom rebars

Table 14 : element force for DP-S1-C-O1

Elem. No.	Force (kN)	Elem. No.	Force (kN)	Elem. No.	Force (kN)	Elem. No.	Force (kN)
1	-34.0	2	16.1	3	-34.0	4	-21.3
5	15.3	6	14.8	7	-21.6	8	-12.6
9	-110.9	10	-111.0	11	-12.2	12	-181.8
13	1.1	14	1.4	15	-165.7	16	-166.8
17	-102.5	18	90.5	19	6.4	20	5.9
21	91.1	22	-103.1	23	-162.6	24	-165.7

25	21.1	26	-121.9	27	-129.5	28	-122.9
29	20.5	30	-97.6	31	0.0	32	168.0
33	-166.5	34	-168.1	35	168.9	36	0.0
37	-98.3	38	10.6	39	10.6	40	295.7
41	12.0	42	12.0				

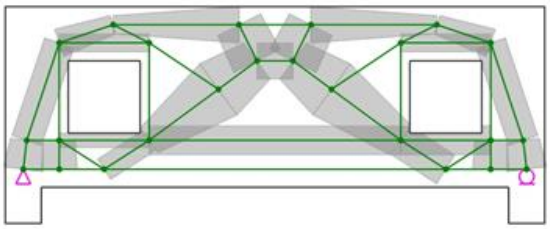

Figure 78 : avalabile width DP-S1-C-O1

4-6-3-1 Concentrated Node

(A) Node 2 (CCT)

Lb = 100.0 mm , ha = 100.0 mm

Lb1 = 0.0 mm , Lb2 = 99.2 mm

F1′ = 33.95 kN , theta 1′ = 0.0 deg.

F2′ = 110.90 kN , theta 2′ = 63.4 deg.

W1,req = 13.9 mm = W1,prov = 100.0 mm (OK)

W2,req = 45.3 mm = W2,prov = 133.4 mm (OK)

Lb,req = 40.8 mm = Lb,req = 100.0 mm (OK)

(B) Node 3 (CCT)

Lb1 = 99.3 mm , Lb2 = 0.0 mm

F1′ = 110.98 kN , F2′ = 34.00 kN

theta 1′ = 63.4 deg. , theta 2′ = 0.0 deg.

W1,req = 45.3 mm = W1,prov = 133.5 mm (OK)

W2,req = 13.9 mm = W2,prov = 100.0 mm (OK)

Lb,req = 40.8 mm = Lb,req = 100.0 mm (OK)

Pn	98.3	kN
2Pn (P_{STM})	197	kN
P_{ABAQUS}	199	kN
P_{STM} / P_{ABAQUS}	0.989	

Failure occurred due to the yielding of the tension ties

BEAM #.	Specimen Designation	ABAQUS Failure load (KN)	Strut and Tie Failure load (KN)	P_{STM} / P_{ABAQUS}
1	DP-S1	479	430	0.898
2	DP-S1-F-30	660	610	0.924
3	DP-S1-C-O1	197	199	0.989

4-7 SUMMARY

This chapter studied Strut and Tie and methods of transporting loads in the form of a truss . There are several way to transfer load in each deep beam , the best case gives us a failure load close to the output of the ABAQUS program . We conclude the following from this chapter :
In the case of openings in the deep beam , the behavior and shape of the truss changes in proportion to the openings so that the force moves around the openings .
Strut and Tie is a method that give high freedom to the designer to determine the form of transmission of forces .

Chapter 5: Discussion

5-1 General

The results showed a high convergence between the practical experiment and the abacus program, and based on it, my variables were developed and their results were adopted .

5-2 location of UHPC layer

In this parameter I use two type : * Full grove UHPC layer from two face (1500*500 mm).
* 4 grove layer around opening two from each side with 370*500 mm dimension .
For full face ultimate load increase from 1.25 to 1.47 and for grove layer increase 1.13 to 1.38 . from chart we found that full face gave better result but grove layer is cheaper and gave a good increase in maximum failure load . for example DP-S1-C-O1 full grove face F-30 gave 282 KN (1.42 time of control load 199 KN) and 6.3 mm displacement (for control 4.49 mm) , and grove layer gave 262 KN (1.32 time of control load 199 KN) and 5.2 mm displacement (for control 4.49 mm) .

5-3 Thickness of UHPC layer

Two different thicknesses were used without affecting the dimensions of the deep beam with 20 and 30 mm for full and grove . as a result from charts and tables we found that more thickness of UHPC layer gave increase in ultimate failure load an displacement , then 30 mm layer is better for used for full and grove layer .

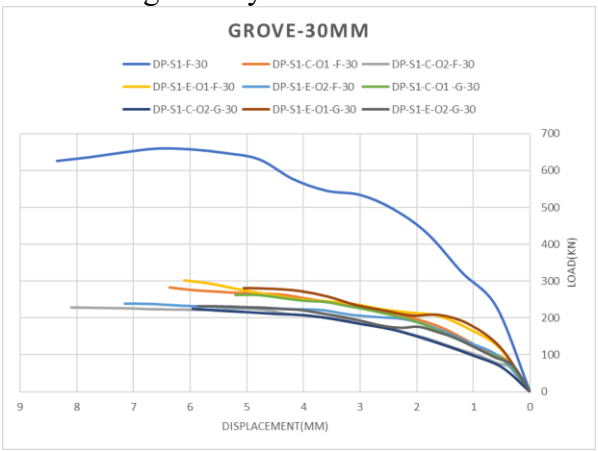

Figure 79 : All beam grove face 30 mm

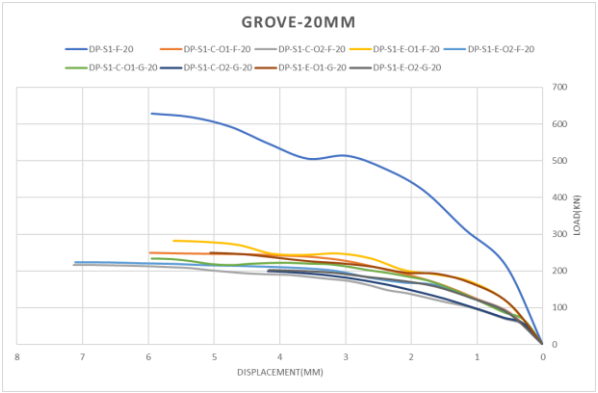

Figure 80 : All beam grove face 20 mm

5-4 Location and dimension of opening

Two type of opening 230*230mm and 200*200mm and location are center of shear span and edge of shear span . as a result of use opening in deep beam we found that increase in opening dimension mean decrease ultimate failure load and increase in displacement , for location of opening at edge is better than at center , the farther we move the opening from shear bath we have increase in ultimate failure load .

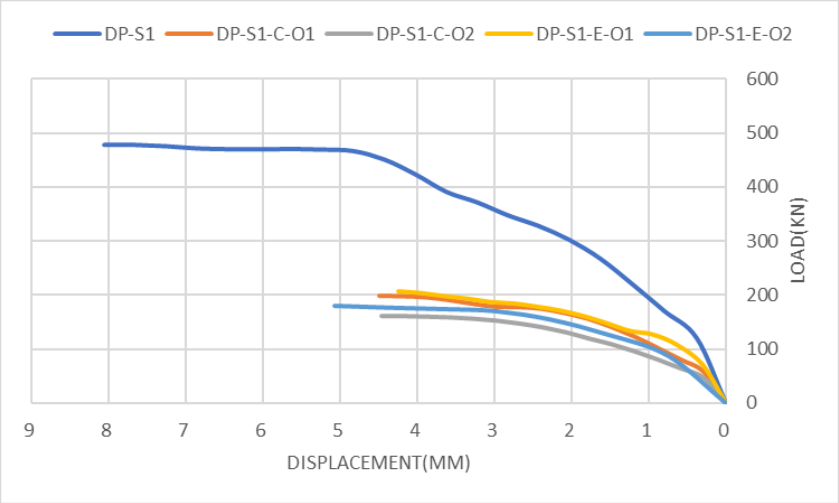

Figure 81 : All beam location of opening

5-5 No shear reinforcement

The shear bars were removed and the effect of strengthening by UHPC was studied for full and grove layer . Some shear rods were kept as a fixation for the flexure bar . after modeling all deep beam and strengthen it with full and grove layer of UHPC 30&20 mm , we found that full face of 30 mm layer from to face without shear gave ultimate failure load and displacement mor than deep beam with shear and no strength . for 30 mm grove layer and no shear ultimate load is 0.88 from the control load and displacement is 0.78 for the control displacement , as a result 20 mm depth is not good enough for strengthen deep beam .

5-6 Strut and Tie

Is one of the variables used to study the behavior of deep beam that are not subject to a Bernoulli theory invalid and known as (Discontinuity region or Deep beam region)

Chapter 6: Conclusion

The following conclusions can be made using the experimental data collected and the evaluation process for various test parameter :

*Deep beams with smaller openings position in shear spans exhibited stiffer behavior than deep beams with bigger openings.

*Deep beam with large opening dimension reduce the ultimate load by 34%–22% compared with deep beams with smaller size openings .

*Displacement for deep beam with opening at edge span is greater than at mid span 15% for the same opening size .

*Used UHPC as strengthen material is good and increase the ultimate failure load 1.13 to 1.46 time , from the control ultimate load

*UHPC layer full face 30 mm grove show increase in ultimate failure load 25%-32% , UHPC layer full face 20 mm grove show increase in ultimate failure load 27%-20% , UHPC layer 370*500*30 mm grove show increase in ultimate failure load 28%-23% , UHPC layer 370*500*20 mm grove show increase in ultimate failure load 11%-19% .

*UHPC layer full face 30 mm grove show increase in mid span displacement 40%-82% , UHPC layer full face 20 mm grove show increase in mid span displacement 32%-60% , UHPC layer 370*500*30 mm grove show increase in mid span displacement 15%-33% , UHPC layer 370*500*20 mm grove show increase in mid span displacement 18%-32% .

* two type of failure for deep beam with web opening (diagonal splitting failure & shear-Compression failure).

* shear bars can replaced by full UHPC layer from two face with 30mm minimum depth and gave more ultimate load and displacement .

*The researchers may receive useful information from the non-linear finite element analysis (FEA) of reinforced concrete members since it is a potent approach. The present work's use of a three-dimensional finite element model makes it possible to forecast how RC solid deep beams and RC deep beams with significant web holes would behave.

* The strut-and-tie method (STM) study of reinforced concrete deep beams revealed a satisfactory correlation with the ABAQUS result, with the discrepancy between the two not exceeding (18%).

Chapter 7: Reference

[1] ACI Committee 318. Building code requirements for structural concrete. ACI 318M-08. Farmington Hills, MI, USA: American Concrete Institute, 2014.

[2] Campione, Giuseppe, and Giovanni Minafò. "Behaviour of concrete deep beams with openings and low shear span-to-depth ratio." Engineering Structures 41 (2012): 294-306.

[3] Altin, S., Anil, ض., & Kara, M. E. (2005). Improving shear capacity of existing RC beams using external bonding of steel plates. Engineering Structures, 27(5), 781–791.

[4] Chen, J. F., & Teng, J. G. (2003). Shear capacity of FRP-strengthened RC beams: FRP debonding. Construction and Building Materials, 17, 27–41.

[5]Li, V. C. (2004). High performance fiber reinforced cementitious composites as durable material for concrete structure repair. Restoration of Buildings and Monuments, 10(2), 163–180.

[6]Al-Osta, M. A. (2018). Exploitation of ultrahigh-performance fibre-reinforced concrete for the exploitation of ultrahigh-performance fibre-reinforced concrete for the strengthening of concrete structural members. Advances in Civil Engineering.

[7]Varghese, P. C., & Krishnamoorthy, C. S. (1966). Streingth and Behaviour of Deep Reinforced Concrete Beams. Indian Concrete Journal, 40(3), 104-108.

[8]Yagendra ,P., (April 1976). Serviceability Considerations for Reinforced Concrete Deep Beams. Journal of Structural Engineering,Vol.4,No.1, ,pp33-38

[9] Kong. F.K (2003). “Reinforced Concrete Deep Beams”, Van Nostrand Reinhold, New York.

[10] [Tuchscherer et al.,2011].

[11] Tan, K., Kong, F., Teng, S., and Guan, L. (1995). “High-Strength Concrete Deep Beams with Effective Span and Shear Span Variations.” ACI Structural Journal, 37(92), 395–403.

[12] Shin, S., Lee, K., Moon, J., and Ghosh, S. K. (1999). “Shear Strength of Reinforced High-Strength Concrete Beams with Shear Span-to-Depth Ratios between 1 . 5 and 2 . 5.” ACI Structural Journal, 61(96), 549–556.

[13] Subedi, N. K., Vardy, A. E., & Kubotat, N. (1986). **Reinforced concrete deep beams some test results**. Magazine of Concrete Research, 38(137), 206-219.

[14] Mohammadhassani, Mohammad, et al. "Ductility and performance assessment of high strength self compacting concrete (HSSCC) deep beams: An experimental investigation." Nuclear Engineering and Design 250 (2012): 116-124.

[15](B.A. Graybeal 2009)[15] من بحثي اليو اتش بي سي طولو.

[16] Lu, W., Lin, I., and Yu, H. (2013). “Shear Strength of Reinforced Concrete Deep Beams.” Aci Structural Journal, 55(110), 671–680

[17] Birrcher, D. B., Tuchscherer, R. G., Huizinga, M., and Bayrak, O. (2013). “Minimum Web Reinforcement in Deep Beams.” ACI Structural Journal, 26(110), 297–306.

[18] Mansur, M. A., and W. A. M. Alwis. "Reinforced fibre concrete deep beams with web openings." *International Journal of Cement Composites and Lightweight Concrete* 6.4 (1984): 263-271.

[19] Mansour, Moustafa, and Tamer El-Maaddawy. "Testing and modeling of deep beams strengthened with NSM-CFRP reinforcement around cutouts." *Case Studies in Construction Materials* 15 (2021): e00670.

[20] Jasim, Waleed A., Yazan B. Abu Tahnat, and Abdulsamee M. Halahla. "Behavior of reinforced concrete deep beam with web openings strengthened with (CFRP) sheet." *Structures*. Vol. 26. Elsevier, 2020.

[21] von Ammon, Ludwig, and Karl Wilhelm ritter von Gümbel. *Wilhelm von Gümbel: ein Nekrolog*. C. Wolf, 1899.

[22] Lampert, Paul, and CEB. "TORSION AND BENDING IN REINFORCED AND PRESTRESSED CONCRETE MEMBERS." *Proceedings of the Institution of Civil Engineers* 50.4 (1971): 487-505.
[23]Schlaich, Jorg, Kurt Schäfer, and Mattias Jennewein. "Toward a consistent design of structural concrete." *PCI journal* 32.3 (1987): 74-150.
[24] Park, J.W.; Kuchma, D. Strut-and-tie model analysis for strength prediction of deep beams. ACI Struct. J. 2007, 104, 657–666.
[25]Lin, I. J., Hwang, S. J., Lu, W. Y. and Tsai, J. T. (2003), "Shear strength of reinforced concrete dapped-end beams", Struct. Eng. Mech., 16(3), 275-294.
[26] Lu, W.Y. and Lin, I. J. (2009), "Behavior of reinforced concrete corbels", Struct. Eng. Mech., 33(3), 357-371.
[27] Karimizadeh, Hamid, and Abolfazl Arabzadeh. "A STM-based analytical model for predicting load capacity of deep RC beams with openings." *Structures*. Vol. 34. Elsevier, 2021.
[28] Tseng, C. C., Hwang, S. J., & Lu, W. Y. (2017). **Shear Strength Prediction of Reinforced Concrete Deep Beams with Web Openings**. ACI Structural Journal, 114(6), 1569-1579.
[29] Tan, K. H., C. Y. Tang, and K. Tong. "Shear strength predictions of pierced deep beams with inclined web reinforcement." *Magazine of Concrete Research* 56.8 (2004): 443-452.
[30] Kong F. K., Sharp G. R., Appleton S. C., Beaumont C. J. and Kubik L. A. Structural idealisation for deep beams with web openings: further evidence. Magazine of Concrete Research, 1977, 30, No. 103, 89–95.
[31] Jung-Woong Park and Daniel Kuchma, "Strut-and-Tie Model Analysis for Strength Prediction of Deep Beams," Structural Journal, V. 104, 2007 PP. 657- 666.
[32] Campione, Giuseppe, and Giovanni Minafò. "Behaviour of concrete deep beams with openings and low shear span-to-depth ratio." *Engineering Structures* 41 (2012): 294-306.
[33] Khalaf, Mohammed Riyadh, and Ali Hussein Ali Al-Ahmed. "Shear strength of reinforced concrete deep beams with large openings strengthened by external prestressed strands." *Structures*. Vol. 28. Elsevier, 2020.
[34] Hamzenezhadi, Abuzar, Mohammad Kazem Sharbatdar, and Ali Kheyroddin. "Experimental investigation of dimensional ratio effects on shear capacity of high-performance cementitious composites deep beams." *Journal of Building Engineering* 43 (2021): 102862.
[35] Hu OE, Tan KH, Liu XH. Behaviour and strut-and-tie predictions of high strength concrete deep beams with trapezoidal web openings. Mag Concr Res 2007;59(7):529–41
[36] Yang KH, Eun HC, Chung HS. The influence of web openings on the structural behavior of reinforced concrete high-strength concrete deep beams. Eng Struct 2006;28:1825–34
[37] Yousef, Ahmed M., Ahmed M. Tahwia, and Nagat A. Marami. "Minimum shear reinforcement for ultra-high performance fiber reinforced concrete deep beams." *Construction and Building Materials* 184 (2018): 177-185.
[38]Rahim, N. I., Mohammed, B. S., Al-Fakih, A., Wahab, M. M. A., Liew, M. S., Anwar, A., & Amran, Y. H. (2020). Strengthening the structural behavior of web openings in RC deep beam using CFRP. *Materials*, *13*(12), 2804.
[39]Abadel, Aref, et al. "Experimental study of shear behavior of CFRP strengthened ultra-high-performance fiber-reinforced concrete deep beams." *Case Studies in Construction Materials* 16 (2022): e01103.
[40] Ismail el-kassas, Ahmed, Hassan Mohammed Hassan, and Mohammed Abd El Salam Arab. "Effect of longitudinal opening on the structural behavior of reinforced high-strength

self-compacted concrete deep beams." *Case Studies in Construction Materials* 12 (2020): e00348.
[41] Kumar, H. G. (2012). **Experimental and numerical studies on behaviour of FRP strengthened deep beams with openings** (Doctoral dissertation, MSc Thesis, National Institute of Technology, Rourkela. Google Scholar).
[42] Jasim, W. A., Allawi, A. A., & Oukaili, N. K. (2018). Strength and serviceability of reinforced concrete deep beams with large web openings created in shear spans. *Civil Engineering Journal*, *4*(11), 2560-2574.
[43] Jasim, Waleed A., Yazan B. Abu Tahnat, and Abdulsamee M. Halahla. "Behavior of reinforced concrete deep beam with web openings strengthened with (CFRP) sheet." *Structures*. Vol. 26. Elsevier, 2020.
[44] Bahraq, A. A., Al-Osta, M. A., Ahmad, S., Al-Zahrani, M. M., Al-Dulaijan, S. O., & Rahman, M. K. (2019). Experimental and numerical investigation of shear behavior of RC beams strengthened by ultra-high performance concrete. International Journal of Concrete Structures and Materials, 13, 1-19.
[45] Mabrouk, Rasha TS, Mahmoud AS Mahmoud, and Magdy E. Kassem. "Behavior of reinforced concrete deep beams with openings under vertical loads using strut and tie model." *Civil Engineering Journal* 7 (2022): 148-170